

**The Development and Use of a Fifteen
Year-Old Equivalent Mathematical Phantom
for Internal Dose Calculations**

R. M. Jones
J. W. Poston
J. L. Hwang
T. D. Jones
G. G. Warner

MASTER

OAK RIDGE NATIONAL LABORATORY

OPERATED BY UNION CARBIDE CORPORATION FOR THE ENERGY RESEARCH AND DEVELOPMENT ADMINISTRATION

DISCLAIMER

This report was prepared as an account of work sponsored by an agency of the United States Government. Neither the United States Government nor any agency Thereof, nor any of their employees, makes any warranty, express or implied, or assumes any legal liability or responsibility for the accuracy, completeness, or usefulness of any information, apparatus, product, or process disclosed, or represents that its use would not infringe privately owned rights. Reference herein to any specific commercial product, process, or service by trade name, trademark, manufacturer, or otherwise does not necessarily constitute or imply its endorsement, recommendation, or favoring by the United States Government or any agency thereof. The views and opinions of authors expressed herein do not necessarily state or reflect those of the United States Government or any agency thereof.

DISCLAIMER

Portions of this document may be illegible in electronic image products. Images are produced from the best available original document.

Printed in the United States of America. Available from
National Technical Information Service
U.S. Department of Commerce
5285 Port Royal Road, Springfield, Virginia 22161
Price: Printed Copy \$5.00; Microfiche \$2.25

This report was prepared as an account of work sponsored by the United States Government. Neither the United States nor the Energy Research and Development Administration/United States Nuclear Regulatory Commission, nor any of their employees, nor any of their contractors, subcontractors, or their employees, makes any warranty, express or implied, or assumes any legal liability or responsibility for the accuracy, completeness or usefulness of any information, apparatus, product or process disclosed, or represents that its use would not infringe privately owned rights.

ORNL/TM-5278

Contract No. W-7405-eng-26

HEALTH PHYSICS DIVISION

THE DEVELOPMENT AND USE OF A FIFTEEN YEAR-OLD
EQUIVALENT MATHEMATICAL PHANTOM FOR INTERNAL
DOSE CALCULATIONS

R. M. Jones, J. W. Poston, J. L. Hwang
T. D. Jones and G. G. Warner

Submitted by R. M. Jones to the Graduate School
of Virginia Polytechnic Institute and State University
in partial fulfillment of the requirements for the degree of
Master of Science

JUNE 1976

NOTICE
This report was prepared as an account of work sponsored by the United States Government. Neither the United States nor the United States Energy Research and Development Administration, nor any of their employees, nor any of their contractors, subcontractors, or their employees, makes any warranty, express or implied, or assumes any legal liability or responsibility for the accuracy, completeness or usefulness of any information, apparatus, product or process disclosed, or represents that its use would not infringe privately owned rights.

OAK RIDGE NATIONAL LABORATORY
Oak Ridge, Tennessee 37830
operated by
UNION CARBIDE CORPORATION
for the
ENERGY RESEARCH AND DEVELOPMENT ADMINISTRATION

DISTRIBUTION OF THIS DOCUMENT IS UNLIMITED

**THIS PAGE
WAS INTENTIONALLY
LEFT BLANK**

ACKNOWLEDGMENTS

The authors wish to express their thanks to Stephen W. Croslin, Conrad B. Jenkins, Douglas C. Smiley, and David S. Wagner whose assistance in the early stages of this research was invaluable. We are grateful to Dr. A. K. Furr, Dr. H. A. Kurstedt, and especially Dr. D. B. Rivers for their willingness to assist at the occurrence of any type of difficulty.

We are indebted to Dr. E. M. Smith for his provision of the biological model for dose calculations.

This research was performed in the Health Physics Division of the Oak Ridge National Laboratory, operated for the U.S. Energy Research and Development Administration by the Union Carbide Corporation. For the use of this facility and the assistance given by many of the staff there, we are grateful.

Ms. Kay M. Branam and Ms. Nancy L. Barringer deserve a special thanks for their preparation of the final manuscript, as does Mr. J. P. Hickey for his work in preparing the figures.

**THIS PAGE
WAS INTENTIONALLY
LEFT BLANK**

THE DEVELOPMENT AND USE OF A FIFTEEN YEAR-OLD
EQUIVALENT MATHEMATICAL PHANTOM FOR INTERNAL
DOSE CALCULATIONS

Abstract

The existence of a phantom based on anatomical data for the average fifteen year-old provides for a proficient means of obtaining estimates of absorbed dose for children of that age. Dimensions representative of an average fifteen year-old human, obtained from various biological and medical research, were transformed into a mathematical construct of idealized shapes of the exterior, skeletal system, and internal organs of a human. The idealization for an average adult presently in use by the International Commission on Radiological Protection was used as a basis for design.

The mathematical equations describing the phantom were developed to be readily adaptable to present-day methods of dose estimation. Typical exposure situations in Nuclear Medicine have previously been modeled for existing phantoms. With no further development of the exposure model necessary, adaptation to the fifteen year-old phantom demonstrated the utility of the design. Estimates of absorbed dose were obtained for the administration of two radiopharmaceuticals, ^{99m}Tc -Sulfur Colloid and ^{99m}Tc -DMSA.

**THIS PAGE
WAS INTENTIONALLY
LEFT BLANK**

TABLE OF CONTENTS

CHAPTER	PAGE
I. HISTORY AND PURPOSE.	1
II. MATHEMATICAL PHANTOM	10
Introduction	10
Composition of the Phantom	11
Exterior of the Phantom.	19
Skeletal System.	21
Internal Organs.	27
III. DOSIMETRIC MODEL	32
Introduction	32
Absorbed Dose.	33
Decay Scheme Data.	34
Biological Model	34
Monte Carlo Simulation	37
Estimates of Absorbed Dose	47
IV. CONCLUSION AND RECOMMENDATIONS	49
BIBLIOGRAPHY.	52
APPENDIXES.	56
VITA.	83

LIST OF FIGURES

FIGURE	PAGE
1. The Fifteen Year-Old Human Phantom.	12
2. X-Z Cross Sectional Plots of the Fifteen Year-Old Human Phantom.	13
3. X-Y Cross Sectional Plots of the Fifteen Year-Old Human Phantom.	14
4. X-Y Cross Sectional Plots of the Fifteen Year-Old Human Phantom.	15
5. X-Y Cross Sectional Plots of the Fifteen Year-Old Human Phantom.	16
6. X-Y Cross Sectional Plots of the Fifteen Year-Old Human Phantom.	17
7. X-Y Cross Sectional Plots of the Fifteen Year-Old Human Phantom.	18
8. Idealized Model of the Skeleton for Computer Calculations (left) and a More Realistic Representation (right) with Percentages of Red Marrow Found in the Shaded Portions of the Bones. Clavicles and Scapulae Not Shown In Picture.	23
9. The Internal Organs of the Phantom Plotted from the Equations (left) and Conceptually Drawn (right)	28
10. Schematic Diagram of Nasal Fossa and Brain of the Phantom.	31
11. Isomeric Level Decay of ^{99m}Tc , Decay Data and Equilibrium Dose Constants.	35
12. A Sample Output of GAM-15	42
A-1. Mathematical Models for the Heart, Liver, Brain and Lungs	58
A-2. Mathematical Models for the Thyroid, Testis, Ovaries and Thymus.	60

FIGURE	PAGE
A-3. Detailed View of Scapulae and Clavicles.	63
A-4. Gastrointestinal Tract	66
A-5. Mathematical Models for Bladder, Kidneys, Pancreas, Uterus, Spleen and Adrenals.	69

LIST OF TABLES

TABLES	PAGE
I. External Dimensions of the Fifteen Year-Old Human Phantom.	22
II. Masses of Red and Yellow Marrow and Bone in the Phantom.	25
III. Masses of the Internal Organs of the Phantom.	29
IV. Cumulated Activity for ^{99m}Tc -Sulfur Colloid and ^{99m}Tc -DMSA	38
V. Absorbed Fractions for the Photon Spectrum of ^{99m}Tc for the Fifteen Year-Old Human Phantom	45
VI. Absorbed Dose to Selected Organs from ^{99m}Tc -Sulfur Colloid	46
VII. Absorbed Dose to Selected Organs from ^{99m}Tc -DMSA	48

CHAPTER I

HISTORY AND PURPOSE

The research described herein spans several disciplines and is important to all of them. The research results are important to the field of health physics because the health physicist is charged with the responsibility of protecting man and his environment from the harmful effects of ionizing radiation. The research is important in nuclear engineering because of the high importance of population exposure calculations to the siting of nuclear power reactors and fuel processing facilities. Finally, this research has direct application in nuclear medicine and diagnostic radiology. It is well known the exposure to medical diagnostic x-rays represents the major source of exposure to the population from man-made sources of radiation.⁵²

Thus, a historical foundation for this research would lie probably with Roentgen's discovery of x-rays in 1895. Many date the beginning of diagnostic radiology and radiation protection to this discovery. Not long after his discovery, the biological effects of ionizing radiation became apparent. The French physicist Henri Becquerel had done much work in linking the phenomenon of phosphorescence to x-rays making use of photographic plates. In 1901, after traveling to London to lecture there, he discovered a reddened area on his abdomen. The cause he linked to a sample of radium that he had with him in the pocket directly over the spot. This was one of the first noted signs that these x-rays might have some harmful effect on tissue. It was in 1903 that the American inventor Alexander Graham Bell made the suggestion that sources containing radium might be placed near or in

tumors, for it had been hypothesized that this destructive effect might be more potent interacting with cancerous tissues than with normal tissues.¹ The first ideas that this new discovery of x-rays might be a new type of miracle cure sparked many different forms of serendipitous experimentation. At this time it was hardly thought that the small amounts of radium being used on humans would have any harmful effects biologically. A statement dealing with the biological effects of radium appearing in the 1916 journal Radium, stated that radium has absolutely no toxic effects, it being accepted as harmoniously by the human system as is sunlight by the plant.²

During this "classical" period, the physicists attempted to learn more about the atom and its radiations. In addition, the instrumentation for detection and measurement of these radiations was being developed. Rutherford utilized a photographic plate and in 1903, Crookes' invention of the spintharoscope marked the opening of the development of the scintillation detector. The invention of the cloud chamber and gold leaf detectors also played major roles. A culmination of much of the knowledge gained in this period can be found in the perfection of the Geiger counter in 1928.¹

The improvement in instrumentation opened the door for the use of radioisotopes as tracers. The first of these experiments was performed by the Hungarian chemist Hevesy in 1923. He utilized an isotope of lead to investigate the metabolism of lead in plants using a very sensitive gold leaf detector. He was a pioneer in this field, defining many of the basic principles of tracer technology in use today.³ By the late twenties, clinical studies using radioactive injections, such

as the determination of the mean arm-to-arm circulation time, were well underway.¹

The transition from the "classical" period into the "modern era" was seeded early in 1919 by Rutherford's discovery that the structure of matter could be changed by bombardment with alpha particles from radium. It was the ingenious work of Ernest O. Lawrence in the development of the cyclotron in 1931⁴ and the experimentation of Irene Curie and Frederic Joliot in 1934, showing the mutation of some light elements to radioactive forms of other elements by neutron bombarding,⁵ that clearly marked the end of the "classical" period. Artificially produced radioisotopes began to emerge slowly from all parts of the world. Lawrence and his brother John produced a large cyclotron that they called "The Medical Cyclotron".⁴ Hevesy and his colleagues with the use of a Geiger counter and ³²P as sodium phosphate, determined that bone formation in the rat is a dynamic process.⁶ In 1936, John Lawrence used the same radionuclide as a phosphate in the treatment of leukemia.¹ Therefore, two of the most important studies in nuclear medicine were underway in 1936; the study of the dynamic state of body constituents and therapeutic uses of radioisotopes.

During this same transitional period there were recommendations for protection against the hazards associated with the radiation and the use of radioisotopes. It was 1916 before organized efforts for methods of radiation protection came into existence. However, good recommendations from individuals came as early as 1902 when Rollins suggested the use of x-ray film as a means of monitoring exposure.⁷ The recommendations were exactly that and not enforceable laws. They

were based on qualitative measures which made any estimation of dose far from precise. For example, in 1925, Mutscheller made recommendations that the limit of protection should be 1/100 of an erythema dose in 30 days.⁸ The reddening of the skin was used as an indicator of dose and the theory was that there was a threshold level of exposure below which one could receive radiation and tolerate it without ultimately suffering injury. Thus, the term "tolerance dose" was used widely in the field. The estimation of dose to tissues from external sources in this early period, was more an artistic evaluation than a science. It is important to note also that the estimation of dose from internal sources was non-existent. The adoption of the Roentgen as the standard unit of exposure by the International Commission on Radiological Units (ICRU) in 1928 marked the beginning of efforts to quantify dose estimations as measures of exposure.⁷ The ICRU, 1925, and the International Commission on Radiological Protection (ICRP), 1928, were established by the International Congress of Radiology. In 1929, the National Committee on Radiation Protection and Measurements (NCRP) was formed in a close relationship with the ICRP and has maintained that closeness to the present. For the first two decades of their existence, both the ICRP and the NCRP were concerned primarily with recommendations of maximum permissible exposures from x-rays and radium.⁹

The introduction of the first nuclear reactor on December 2, 1942, marked the beginning of the "modern" era for all fields associated with radioactivity. The change was exemplified in the first use of the word "Health Physics" for the whole of radiation protection and all its

associated activities.¹⁰ The discoveries made in the "classical" period became dynamic in their growth. The change is due largely to the efforts of Enrico Fermi and his colleagues. In 1946 artificially produced radioisotopes were made available to the public and as a result of the advances in technology and physics, were soon tailor-made for use in medicine. Some of the isotopes produced in the early period were not put to specific use until advances in instrumentation and pharmacology made their use feasible. The field of nuclear medicine has become so advanced with sophisticated scanning instrumentation, advances in and methods of tracers in diagnosis and treatment, that today subspecialties are appearing such as cardiovascular, endocrinologic pulmonary and pediatric nuclear medicines.¹

In 1946 the NCRP realized a need for reorganization and growth to meet the needs of the problems associated with the progress in all fields of radioactivity.⁴ Four years later, the ICRP underwent a similar change. Since 1944 the use of maximum permissible dose (MPD) as a standard for recommendations of exposure limit largely replaced the use of tolerance dose. From more recent analysis it appears that certain types of damage such as the shortening of the life-span, leukemic incidence, and genetic changes increase monotonically with dose, thus contrasting the theory of a threshold.¹² This would suggest that any amount of radiation exposure, no matter how small, is potentially harmful. Whether or not there exists a threshold for radiation exposure below which no harmful effects would be encountered still remains in debate. However, at this point one finds a change in the attitude of the recommended allowable exposures in that the

attitude is now one of risk versus benefit. The Federal Radiation Council (FRC) was formed in 1959 in the United States to provide policy on human exposure to ionizing radiation. Their attitude toward the setting of allowable standards was expressed formally in 1961.

"...the establishment of radiation protection standards involves a balancing of the benefits to be derived from the controlled use of radiation exposure. The principle is based upon the position adopted by the Federal Radiation Council that any radiation exposure of the population involves some risk; the magnitude at which increases with the exposure."¹³

This attitude is very much the same as that of both the NCRP and the ICRP. In practice, the FRC has closely followed the advice of both of the Commissions in setting standards of exposure.

In the estimation of risk, one must depend on a correlation of the amount of exposure with the potential damage. Usually these correlations are presented in terms of a response versus absorbed dose. There are many problems associated with an attempt to formulate such a relation. Casual relations between radiation exposure and deleterious effects, except for massive acute exposures, can only be established statistically. The induced biological effects of radiation do not appear to be unique. Secondly, there are sometimes long periods of time before effects are noticeable. In addition, there are only approximate ways to calculate the absorbed dose to tissues, for the calculations depend on numerous variables. As a result, there are several correlation curves that may represent the true response versus absorbed dose relation. The most conservative position to take would be to assume a linear relation without a threshold at low exposures. This, therefore, is the position that has been taken by the ICRP and NCRP.¹²

The basis of sound estimation of risk involves a precise estimation of absorbed dose. The absorbed dose, however, is dependent on such parameters as the nature of the exposure, whether internal or external, the energies of the emitted particles and the physiologic factors of the system encountered. In 1949 a group of concerned health physicists from the United Kingdom, Canada, and the United States agreed to gather the necessary information to formulate a "Standard Man" as a typical radiation worker.¹¹ From that time there have been various mathematical and experimental efforts to estimate absorbed dose to various tissues of an "average" adult. The most sophisticated methods are those associated with the efforts of the ICRP, NCRP, and the Medical Internal Radiation Dose Committee (MIRD) of the Society of Nuclear Medicine. Organized efforts to formulate the "Standard Man" are culminated in the ICRP Publication, Report of the Task Group on Reference Man.¹⁴ This report represents a detailed analysis of anatomical data, elemental composition of various tissues and organs, intake of air, water, and other elements, and data on excretion.

In nuclear medicine the administration of radionuclides to various age groups has increased. The diagnostic use of x-rays has broadened to include all age groups and accounts for a major portion of the increase in external exposure to the general population. These increases in exposure to radiation dictate the need for precise estimates of absorbed dose. An effort to do so came in 1967 when Fisher and Snyder completed the design of a detailed mathematical phantom based on the anatomical values outlined by the Task Groups of the ICRP as being representative of an "average adult."¹⁵ Since that

time, revisions in the model have been made and published by Snyder et al. in 1974.¹⁶ Though other phantoms have been used in this country and other countries, the MIRD Committee and the ICRP have chosen this particular idealization of the "average adult" for use in dose estimates for various age groups. Five smaller phantoms have been formed by "scaling down" the adult by proper constants.¹⁷ The use of these small adults in dose estimations has been recognized to be a first order approximation. Recently, anatomical data has been used to develop mathematical phantoms that better represent the "average" one year-old and five year-old humans.¹⁸ Though organ shapes remain similar to the adult phantom, physiological geometries of the children phantoms differ from the "scaled down" phantoms. Preliminary results indicate that the dose estimates obtained in these more advanced phantoms are different from those obtained in the "scaled down" phantoms.

In order to improve present estimates of dose to various age groups, the purpose of this research was to develop a fifteen year-old equivalent mathematical phantom based on anatomical data. The phantom was to be designed so that it was consistent with the adult and children phantoms in existence. Therefore, the idealization of most organ shapes were similar to that of the adult. In addition the equations describing the two phantoms were similar. In order for the design of the fifteen year-old phantom to be one of utility, it was necessary that it be readily adaptable to present-day methods of estimating dose. To demonstrate this utility, the phantom was used in a computer simulation of a typical situation in pediatric nuclear

medicine from which estimates of dose to certain organs were calculated. The models and techniques used in the estimation of dose have been adopted in their entirety. It has not been the purpose of this research to improve upon or justify the reported accuracy of these methods, but rather to demonstrate the adaptability of the fifteen year-old phantom design to these methods. Therefore, the major contribution of this research has been the design of the fifteen year-old mathematical phantom, for no other anatomically based idealization of a fifteen year-old human is in existence for purposes of estimations of absorbed dose.

CHAPTER II
MATHEMATICAL PHANTOM

Introduction

After obtaining the necessary anatomical dimensions, these data must be transformed into a set of mathematical equations which, consistent within themselves, form a phantom similar in shape to an "average" human being of a certain age. This mathematical construct must have organs similar in shape to those organs of a human. The organs must not intersect at any point and must remain within the constraints of the exterior equations. In addition these organs must be placed within the boundaries in such a manner as to resemble their positioning within the human body. The Snyder and Fisher phantom accomplishes these tasks successfully for the adult.¹⁶ This phantom is the most detailed mathematical design of the human adult for purposes of dose estimations in use at the present time. For this reason it was decided to employ anatomical data for the fifteen year-old in a manner similar to that used by Fisher and Snyder to construct the average adult.

In Chapter I, it was stated that the Snyder-Fisher phantom, (previous reference to this phantom has been as the adult phantom), has been shrunk by constant factors to form a fifteen year-old phantom. One should be aware of the differences resulting in this type of formation of a fifteen year-old phantom and the formation using anatomical data. For instance, the thymus is larger in a fifteen year-old human than in an adult. If the adult phantom is shrunk to create a younger phantom, the thymus will be smaller than the adult and would

not correspond to that of a fifteen year-old. Though the overall weight and height of the fifteen year-old will be less, the relative size of the organs may differ and can be determined only by referring to actual anatomical data.

To describe the phantom in Figure 1 requires a large number of equations. Although these mathematical descriptions represent the major contribution of the research, they have been placed in explicit form in Appendix A. The phantom is placed in a rectangular coordinate system with the origin at the center of the base of the trunk. The positive Z-axis points upward toward the head, the positive X-axis is directed toward the reader's right and the phantom's left, and the positive Y-axis is directed out the rear of the phantom. The equations were plotted on a calcomp plotter to check for errors, intersections of organs, shape and location. The results are in Figure 2 through Figure 7. Both X-Y and X-Z cross sectional plots are shown and, combined with the other figures, give a pictorial image of the mathematical construct.

Composition of the Phantom

To transform the data on body and organ masses into mathematical equations, one must obtain a value for the density of the medium. The total volume of the phantom was determined using a specific gravity specified for fifteen year-old humans. However, the density alone is not sufficient to carry out the calculations of absorbed dose. The elemental composition of the phantom must be determined. Photon interaction cross-sections are an integral part of the photon transport code. These cross-sections are determined based on the elemental

ORNL-DWG 72-12864R1

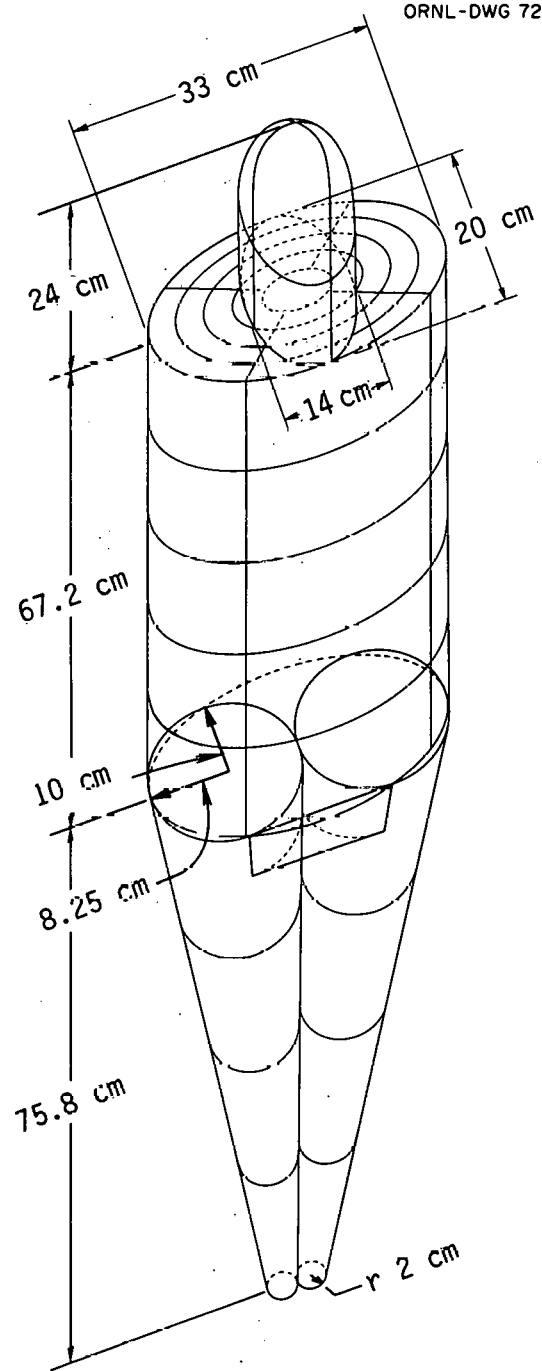


FIGURE 1. THE FIFTEEN YEAR-OLD HUMAN PHANTOM.

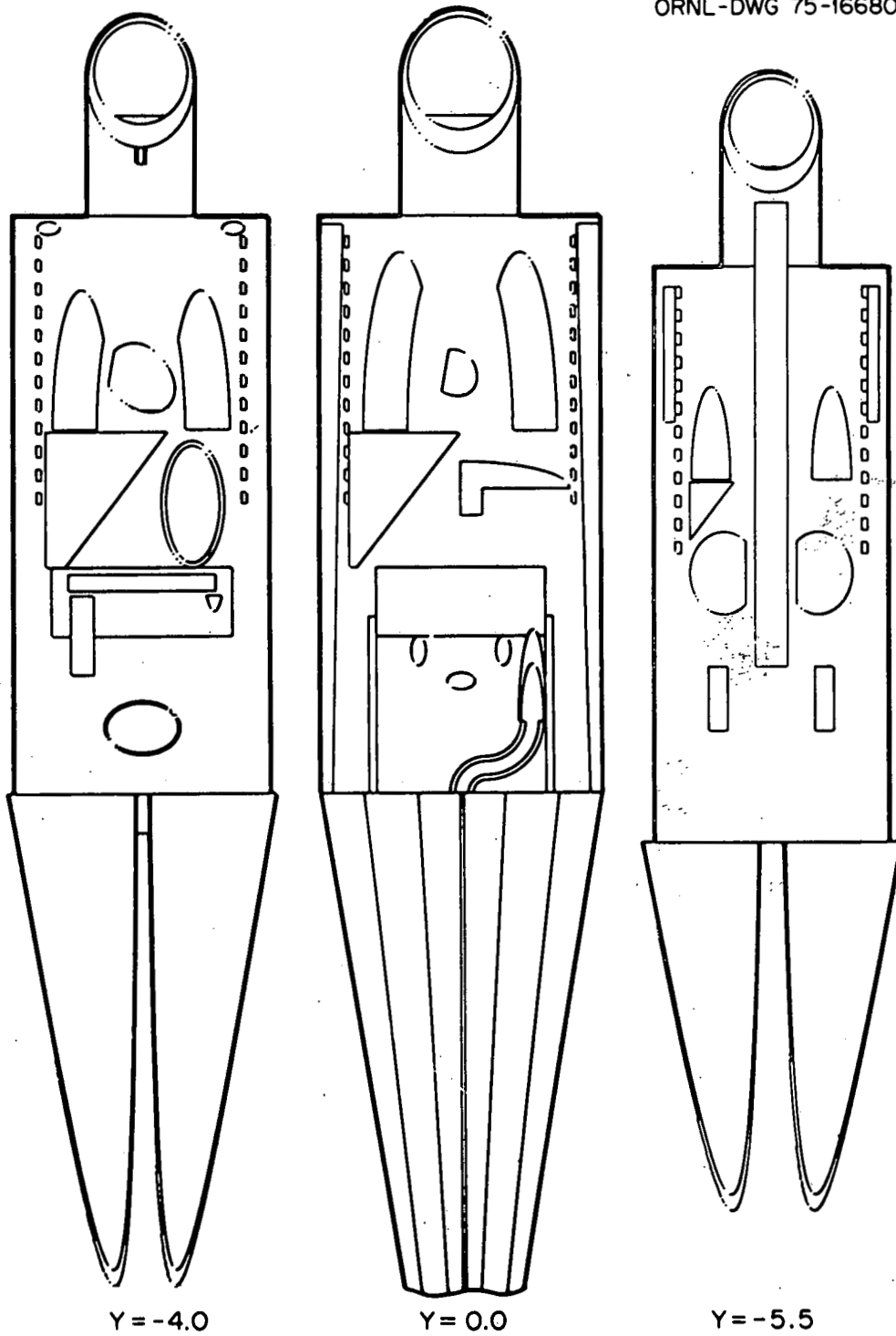


FIGURE 2. X-Z CROSS SECTIONAL PLOTS OF THE FIFTEEN YEAR-OLD HUMAN PHANTOM.

ORNL-DWG 75-16681

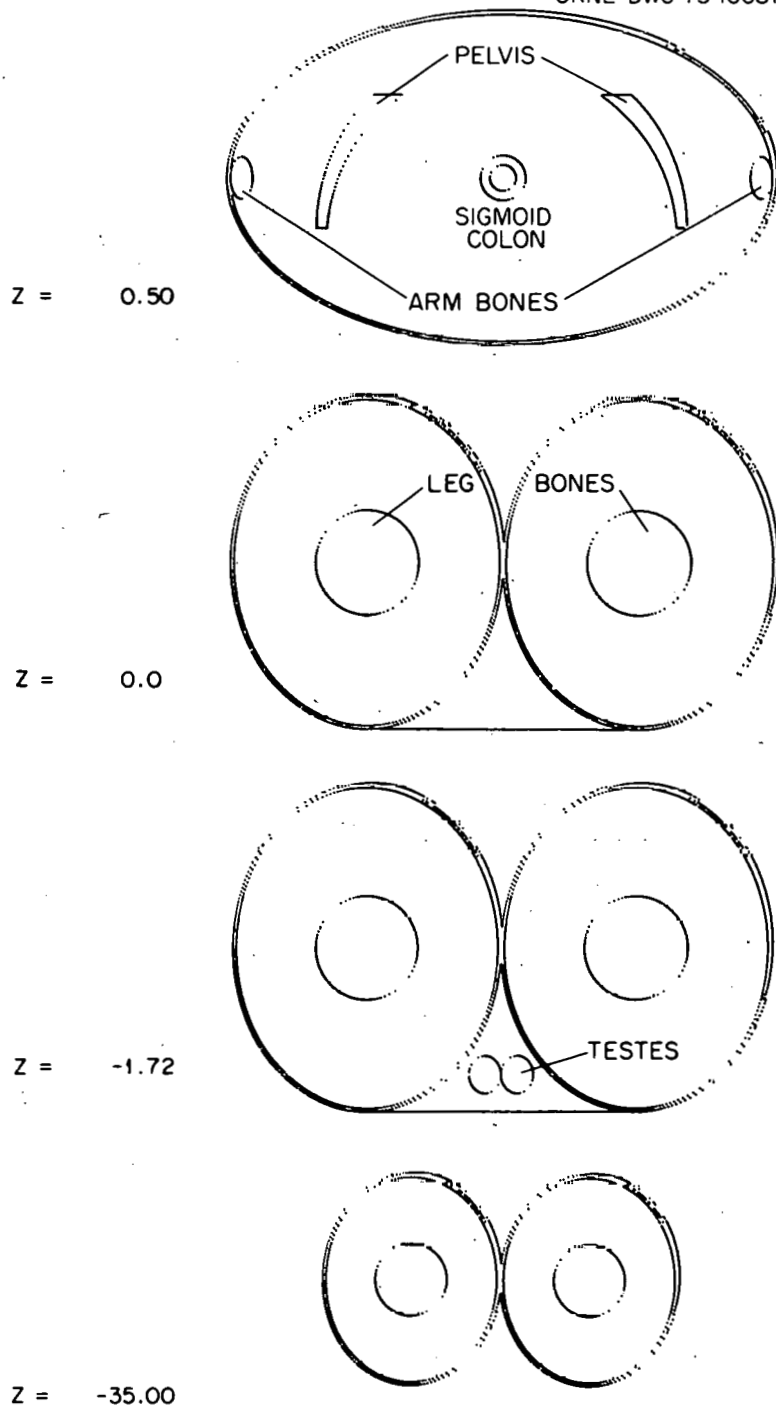


FIGURE 3. X-Y CROSS SECTIONAL PLOTS OF THE FIFTEEN YEAR-OLD HUMAN PHANTOM.

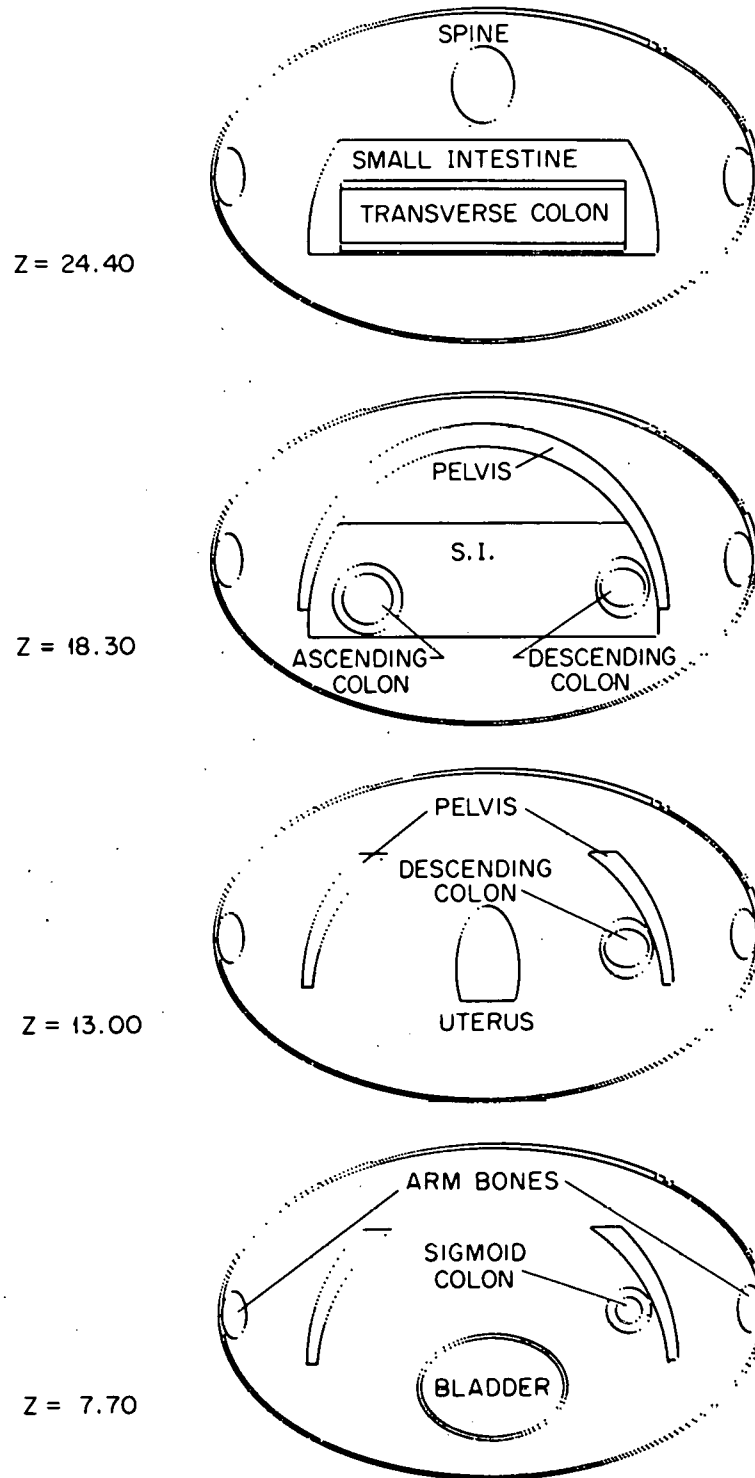


FIGURE 4. X-Y CROSS SECTIONAL PLOTS OF THE FIFTEEN YEAR-OLD HUMAN PHANTOM.

ORNL-DWG 75-16683

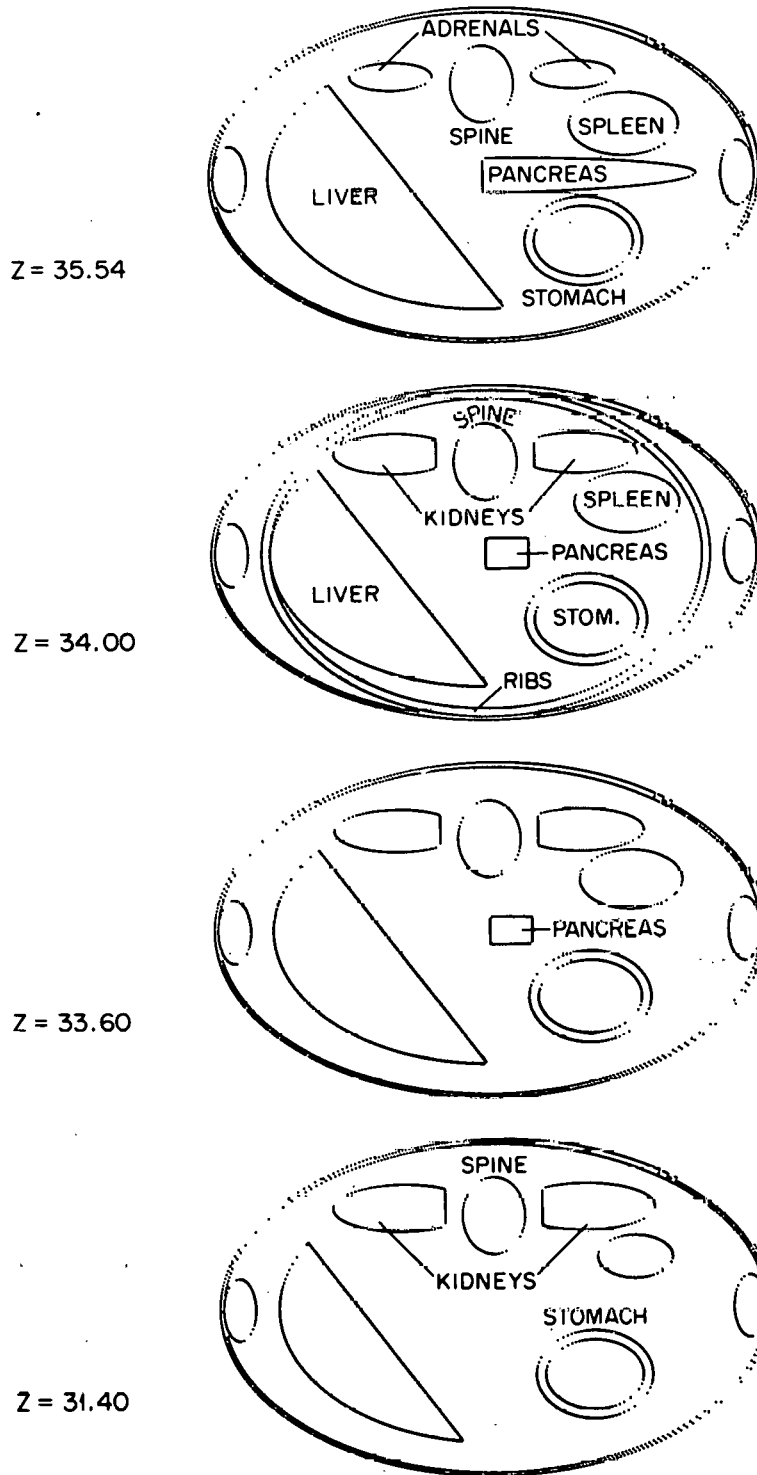


FIGURE 5. X-Y CROSS SECTIONAL PLOTS OF THE FIFTEEN YEAR-OLD HUMAN PHANTOM.

ORNL-DWG 75-16684

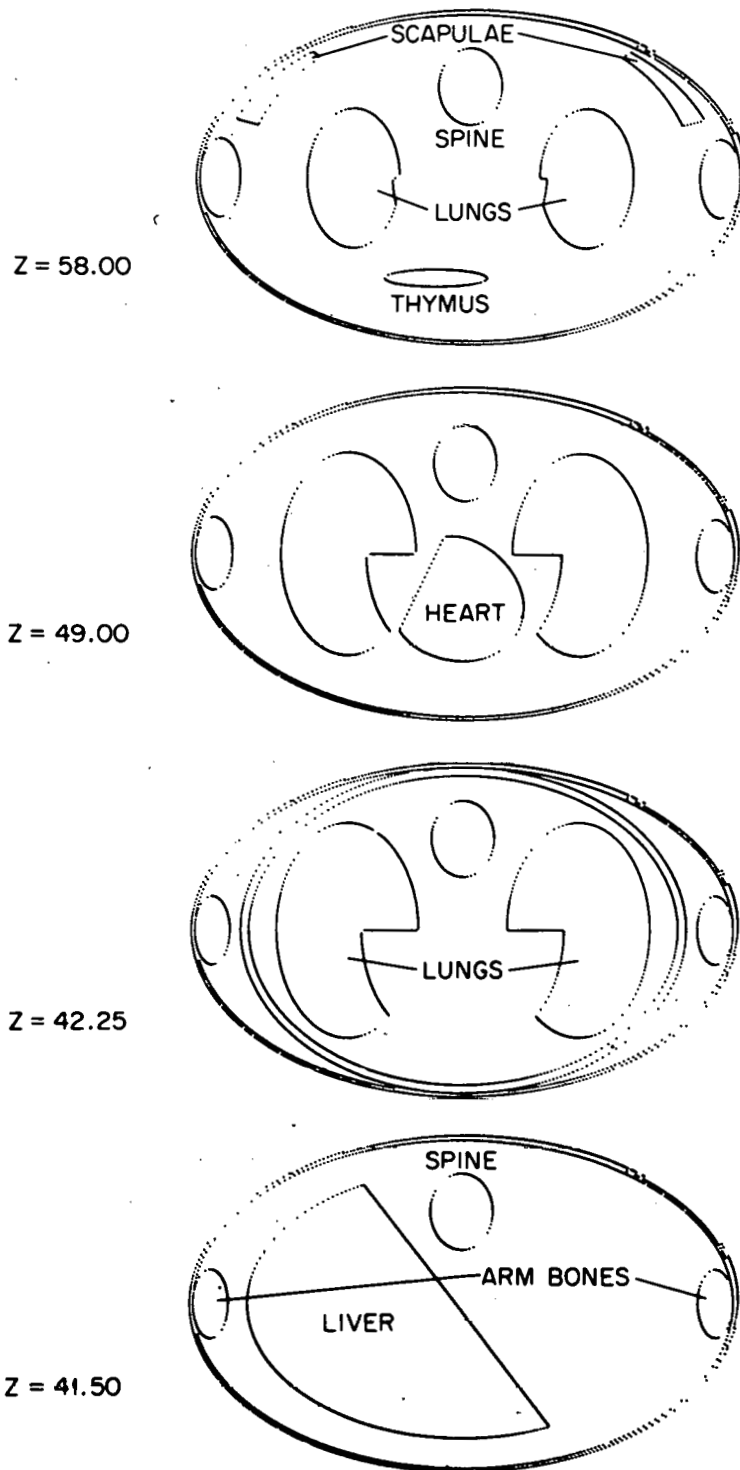


FIGURE 6. X-Y CROSS SECTIONAL PLOTS OF THE FIFTEEN YEAR-OLD HUMAN PHANTOM.

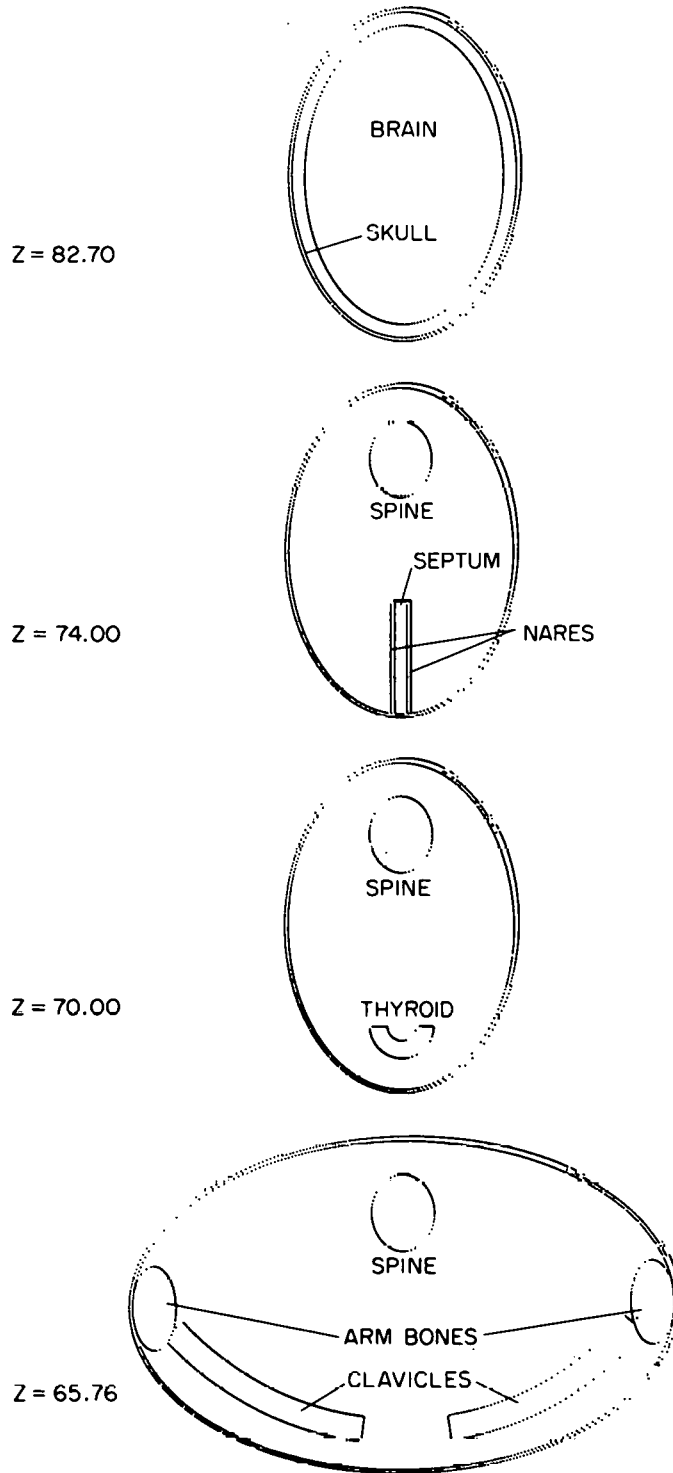


FIGURE 7. X-Y CROSS SECTIONAL PLOTS OF THE FIFTEEN YEAR-OLD HUMAN PHANTOM.

composition of the medium through which the photons are assumed to pass. In 1966, Tipton et al. published values for composition based on the analysis of tissue samples from autopsies of 150 grossly normal U.S. adults.¹⁹ Fisher and Snyder used the results of this study to divide the adult phantom into three regions with different densities: (1) the skeleton; (2) the lungs; and (3) the remainder of the phantom which was considered to be soft tissues. Data of this nature was sparse for age groups other than the adult. Therefore, the composition for the regions of bone, lungs, and tissue in the adult phantom, have been used for the fifteen year-old phantom. The densities of these regions are 1.4826 g/cm³, 0.3 g/cm³, and 0.9869 g/cm³ for the skeleton, lungs and tissue respectively.

Exterior of the Phantom

The weight of an average fifteen year-old has been reported by several authors and ranges between 52 to 61 kg. A total body weight of 58 kg was chosen as a design basis for the phantom. This was an average value of the data, which included a study of 300 healthy Californian children.²⁰ Similarly, for the total body height, one finds a range from 161 cm to 173 cm. The phantom design height was chosen to be 167 cm. This value was 96% of the adult phantom height and was a representative percentage of adult height for fifteen year-olds. Formulae given by Boyd,²¹ for different age groups and different statures, were used to determine the specific gravity. An average specific gravity of about 1.03 was selected. Though this appears to be much higher than the overall density of the adult phantom of 1.004 g/cm³, this value is comparable to the values assigned to the male and

female adults of 1.07 and 1.04 respectively in The Report of the Task Group on Reference Man.¹⁴ It is important that the total volume of the phantom be based on anatomical data. Therefore the determination of this parameter was made assuming a total body weight of 58 kg and a specific gravity of about 1.03. The use of an average total body weight that is possibly more than "normal" is a result of the realization that upon adoption of the three regional compositions, the final phantom mass would be less than the design basis. It was desirable that a phantom total body weight be obtained that is reasonable while holding the total volume constant.

While linear measurements of the body change rapidly from one individual to the next, the relative volume a section occupies is a more slowly varying function. The relative volume of various sections of the body as a function of age can be obtained from a study of Bardeen.²² The phantom has three principal regions: (1) the head, (2) the trunk, and (3) the legs region. These regions do not correspond exactly to an anatomical counterpart. For example, the head region contains both the head and the neck, and the ears and nose are considered negligible. The trunk contains not only the trunk, but the arms as well, with the hands and fingers included in the arm mass. The feet and toes are treated similarly and are included in the legs region. The genitalia region has no real anatomical counterpart, but is constructed to house the testicles in tissue and allow for proper positioning. In most cases the testicles are considered to be a part of the legs region. Using the data from Bardeen²² for a fifteen year-

old, the relative volumes for the phantom head, trunk, and legs region are 8%, 62%, and 30% respectively.

To be consistent with both the anatomical data and the existing adult and children phantoms, the head volume of the fifteen year-old was chosen to be the same as the head volume of the adult. Thus, the anterior to posterior diameter of the trunk section was set at 20 cm. Anatomical data from Pryor²³ supports the choice of 20 cm as dose data from The Report of the Task Group on Reference Man¹⁴ (sagittal diameter at the thorax of about 19 cm).

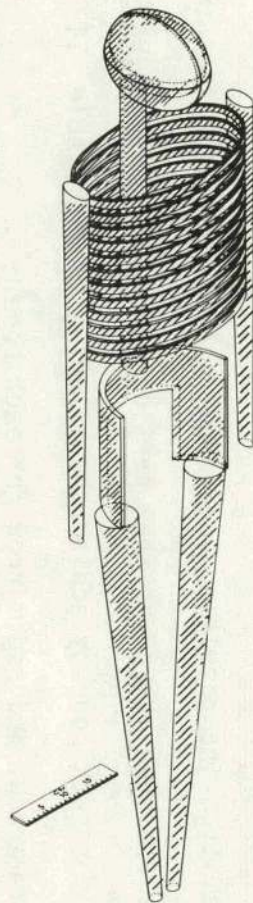
At this point, the remaining external dimensions were adjusted within geometrical and anatomical constraints to achieve a consistent phantom design. The resulting dimensions are given in Table I. The equations for the exterior of the phantom are explicitly given in Appendix A. Note that the leg region of the phantom differs slightly in general description from that of the adult phantom. The upper cross-sectional areas of the legs are elliptical in this design with the major axis in the anterior to posterior direction, whereas the adult design exhibits circular cross sections. Both designs have circular cross sectional areas at the bottom of the legs.


Skeletal System

The model for the skeletal system, shown in Figure 8, assumes a homogeneous mixture of bone and bone marrow. Though it appears to be a simple model, the individual masses required for the design are scarce. Data giving the mass of the entire skeleton as a function of age are available. The nature of these data depends on a number of things, such as the manner in which the skeleton was prepared for

TABLE I
EXTERNAL DIMENSIONS OF THE FIFTEEN YEAR-OLD HUMAN PHANTOM

Total Mass	56,980 g
Total Volume	56,272 cm ³
Total Height	167 cm
Circumference of Head	54 cm
Length of Head	24 cm
Major Axis of the Head (Y-direction)	10 cm
Minor Axis of the Head (X-direction)	7 cm
Circumference of Trunk	84 cm
Length of Trunk	67.2 cm
Major Axis of the Trunk (X-direction)	16.5 cm
Minor Axis of the Trunk (Y-direction)	10 cm
Length of Legs	75.8 cm
Major Axis of the Upper Legs (Y-direction)	10 cm
Minor Axis of the Upper Legs (X-direction)	8.25 cm
Radius of the Lower Legs	2 cm



SKULL	10.0 %
VERTEBRAE	20.0 %
RIBS + STERNUM	10.0 %
SCAPULAE	4.0 %
HEAD AND NECK OF BOTH ARMS	17.8 %
BOTH CLAVICLES	1.0 %
HEAD AND NECK OF BOTH LEGS	13.2 %
PELVIS	24.0 %
TOTAL AMOUNT OF RED BONE MARROW: 950 g	
 RED BONE MARROW	

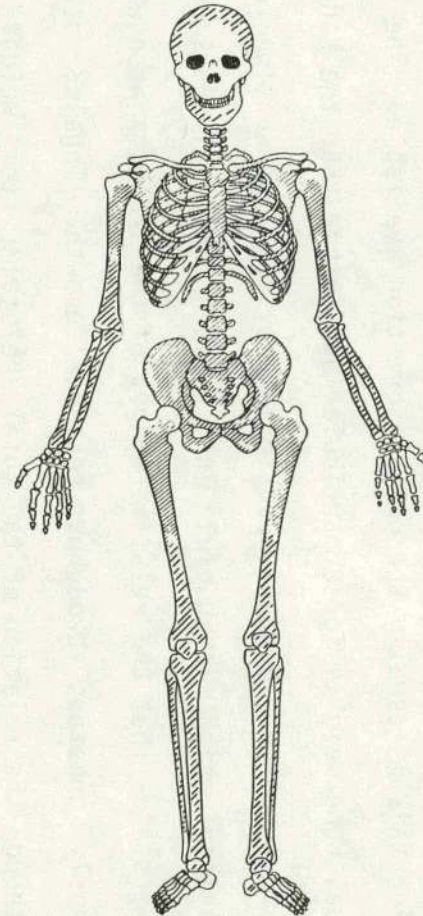


FIGURE 8. IDEALIZED MODEL OF THE SKELETON FOR COMPUTER CALCULATIONS (LEFT) AND A MORE REALISTIC REPRESENTATION (RIGHT) WITH PERCENTAGES OF RED MARROW FOUND IN THE SHADED PORTIONS OF THE BONES. CLAVICLES AND SCAPULAE NOT SHOWN IN PICTURE.

measuring, the state of hydration, the sex, the race, and the original height and weight of the body. These factors are difficult to determine in most studies. However, these data cannot be ignored entirely, for this is usually the only information available. The data on individual bone weights for a particular age, other than the adult, are even more scarce. However, Jackson²⁴ provides a foundation for a general relation which is useful in finding the individual bone weights. He states that the relative weight of the skeleton as a whole remains nearly constant throughout postnatal growth. Ingals²⁵ states that even though the relation of the total skeletal system weight and the total body weight is constant, the individual bone growth is not constant with relation to total body weight.

Assuming that the weight of the skeletal system in a section of the phantom in relation to the weight of the principal section in which it lies remains constant throughout postnatal growth, the simple ratio derived is

$$\frac{\text{Mass of Child Bone}}{\text{Mass of Child Body Section}} = \frac{\text{Mass of Adult Bone}}{\text{Mass of Adult Section}} \quad (1)$$

Precise values of section weights were not known at this point; however, estimates were used based on section volumes and the assumed specific gravity. The resulting individual masses represent the total of the bone and bone marrow in that particular bone. These values can be obtained for each bone by adding the values given in Table II for bone, yellow marrow, and red marrow for each bone.

The bone marrow in the model is divided into two types: (1) red marrow, which is the active marrow; and (2) yellow marrow, which is the

TABLE II
Masses of Red and Yellow Marrow and Bone in the Phantom

Bone Region	Red Marrow (g)	Bone (g)	Yellow Marrow (g)
Arms			
Upper*	28.5	400.2	2.5
Lower	140.3	441.5	177.4
Clavicles	9.5	41.9	16.6
Legs			
Upper**	107.4	445.3	85.7
Lower	18.5	1431.8	227.0
Pelvis	228	163.7	363.3
Ribs	95	574.8	194.1
Scapulae	38	17.5	40.4
Skull			
Cranium***	85.5	533.4	108.9
Mandible	9.5	415.9	10.1
Spine			
Upper [†]	22.7	96.1	32.8
Middle	94.2	466.1	136.1
Lower ^{††}	<u>72.9</u>	<u>77.9</u>	<u>105.1</u>
Total	950.0	6283.1	1500.0

$$* 66.2 \geq z \geq 50.47$$

$$** 0 \geq z \geq -21.6$$

$$*** z \geq -3y + 74.2$$

$$† 67.2 \leq z \leq 74.63$$

$$†† 0 \leq z \leq 33.07$$

remaining bone marrow. Information on the distribution of marrow in terms of absolute masses for individual bones as a function of age is not available. The Report of the Task Group on Reference Man contains data on the mass of the total marrow and the total red marrow as a function of age.¹⁴ Shleien²⁶ discusses the results of Atkinson's work in 1962. Atkinson,²⁶ in deriving an active marrow distribution in various age groups, assumed that: (1) the adult distribution of bone marrow could be used for children; and (b) while active bone marrow distribution varied with age, the distribution of the total marrow remained constant. The red marrow in the fifteen year-old phantom has been distributed from data on the active marrow distribution as a function of age found in Shleien.²⁶ The total marrow, both red and yellow, 2.45 kg, was distributed in the same manner as the adult phantom in all regions excepting the legs region. The marrow allotted to the leg region was not distributed as in the adult for the upper and lower leg regions. In the adult phantom, 2.5% of the total marrow is located in the femora, thus 62.5 grams of total marrow would be assumed to be in the fifteen year-old femora. According to Shleien, there should be 11.3% of the active marrow in these bones; a total of 107 grams of red marrow. The contradiction is obvious. In light of the data from Mechanik,²⁷ the distribution of only 2.5% of the marrow seems too low. Mechanik reports that of the 38.76% of the bone marrow spaces in the body are in the leg region, 17.9% of the spaces are located in the femora. Of the marrow in the legs region, the adult phantom contains 14.2% in the femora and 85.8% in the remaining lower portions. Mechanik concludes that for the bone marrow spaces in the

leg region, 44% are in the femora and 56% are in the lower portions. There are no conclusive studies as to the active marrow and total marrow distributions in the skeleton, especially for the age group of concern. To relieve this contradiction, the adult phantom distribution of total marrow remains constant in the legs region, but this marrow is divided according to the percentages of bone marrow spaces in the upper and lower regions determined by Mechanik. The resulting distribution of active marrow is given in Figure 8 and the absolute values of red marrow, yellow marrow and that which remains as bone are tabulated in Table II.

Internal Organs

Anatomical data were more readily available for the internal organ masses shown in Figure 9. In formulating the design masses given in Table III only one assumption was made. Though an anatomical value was obtained for the total mass of the intestines as a whole there have been no studies concerned with the individual weights of the intestines as a function of age. A study by Underhill²⁸ shows the weight of the intestines to be a function of body size rather than age. If this is the case, a simple weight ratio can be formed as in the derivation of the skeletal system. Again the distribution of the total mass remains the same as in the adult phantom.

In the design of the fifteen year-old the general shape of each organ remained the same as in the adult. However, a special modification was made in the head region. The brain of the adult phantom was defined as the volume of an ellipsoid. The fifteen year-old phantom's brain is also defined by an ellipsoid, but is cut by a

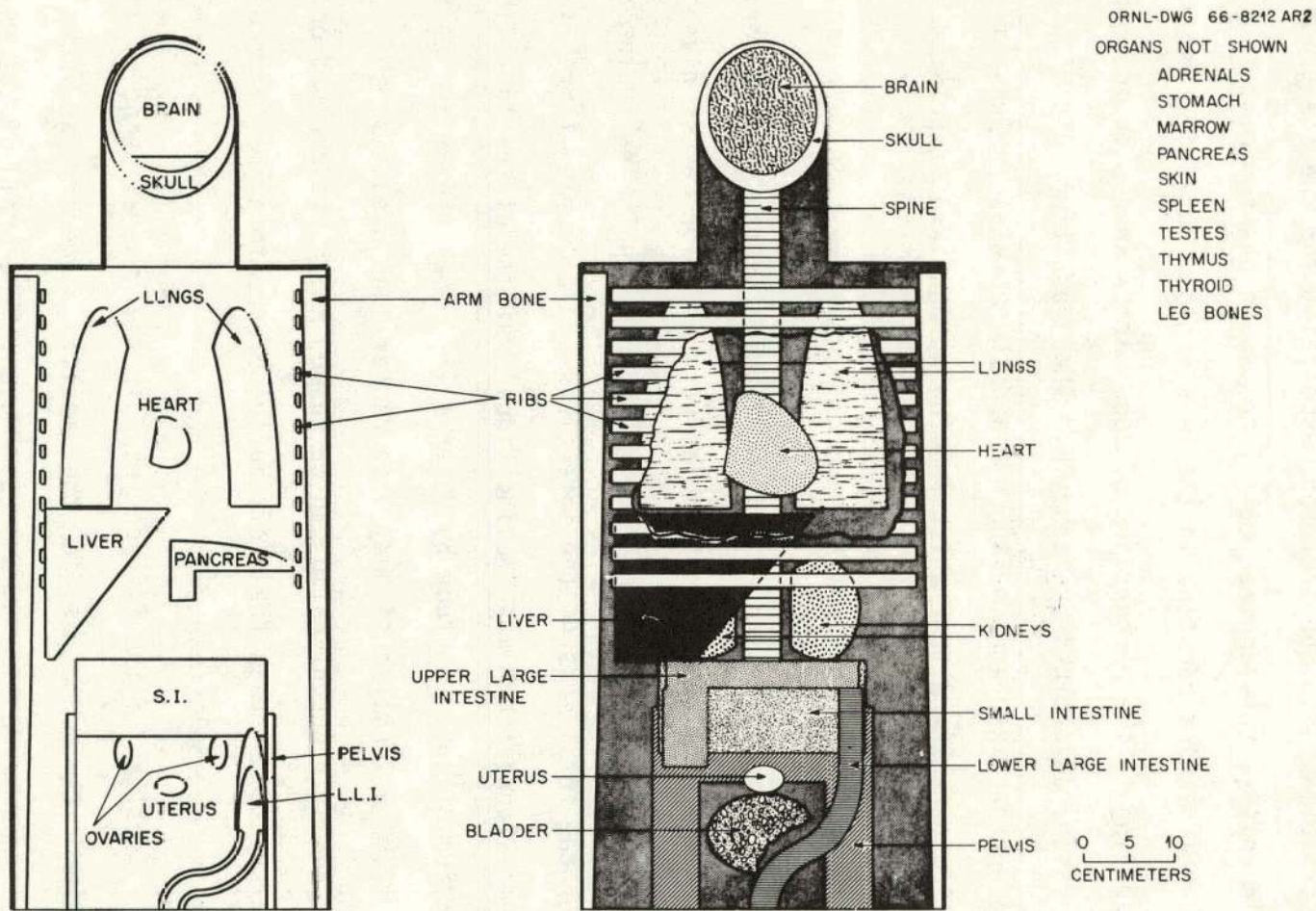


FIGURE 9. THE INTERNAL ORGANS OF THE PHANTOM PLOTTED FROM THE EQUATIONS (LEFT) AND CONCEPTUALLY DRAWN (RIGHT).

TABLE III
 Masses of the Internal Organs of the Phantom

Organ	Mass (g)	Reference
Adrenals	9.1	14, 41, 22
Bladder (wall)	34.5	14
Brain	1344.2	14, 41, 42, 43, 44
G.I. Tract		14, 28, 16
Stomach (wall)	116.3	
S.I. (wall and contents)	742.7	
U.L.I. (wall)	146.3	
L.L.I (wall)	111.1	
Heart	237.9	14, 41, 42, 43, 45, 46
Kidneys	233.1	14, 41, 42, 47
Liver	1267.5	14, 41, 42
Lungs	650.2	14, 42, 45, 48
Nasal Region	23.7	
Ovaries	5.2	14, 41, 49
Pancreas	56.4	14, 42
Spleen	141.5	41, 42, 50
Thymus	27.0	14, 41, 42, 46
Thyroid	13.2	14, 42, 46, 51
Testes	15.6	14, 41, 42, 49
Uterus	28.8	14

plane on the bottom. This shape was chosen as a better approximation of the real brain (seen in Figure 10). A nasal region has also been included. This special region was not included in the published version of the adult phantom,¹⁶ but was added to the adult construct in the computer codes as a source region only. The nasal region was included here to facilitate future calculations. Explicit equations describing these two regions can be found in Appendix A and in Figure 2 and Figure 7.

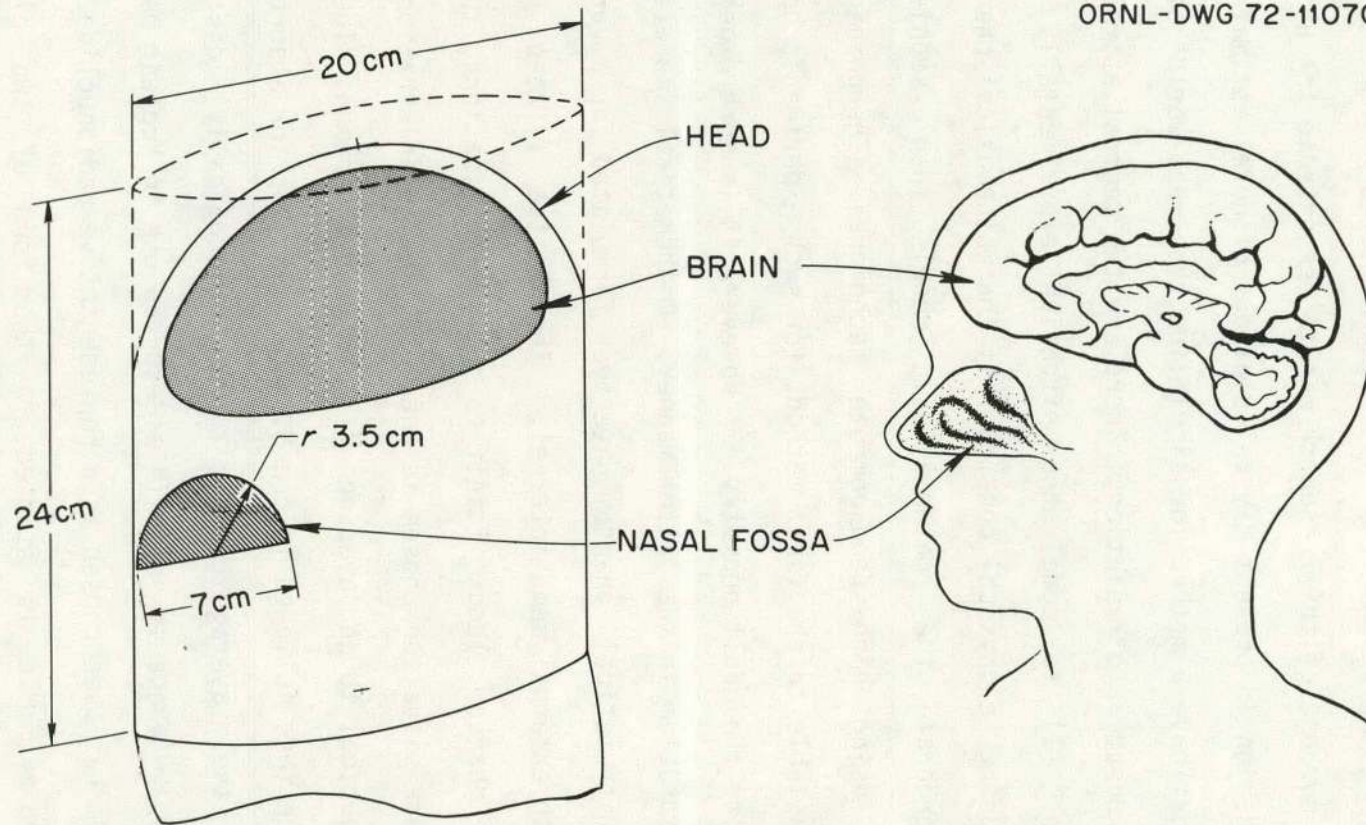


FIGURE 10. SCHEMATIC DIAGRAM OF NASAL FOSSA AND BRAIN OF THE PHANTOM.

CHAPTER III
DOSIMETRIC MODEL

Introduction

Another purpose of this research was to demonstrate the utility of the phantom design in present day calculations of dose estimates. To do so, one must have a method for simulating the "real world" situation of human exposure to radiation. There are two general approaches to this problem: (1) to model the situation experimentally in the laboratory using a physical construct of the mathematical phantom; or (2) to incorporate the mathematical model into sophisticated calculations using high-speed computer techniques. The phantom model is easily adaptable to the first method, for such experiments have been performed using the adult geometry.²⁹ However, it is more expedient to approach the problem in the latter manner. Mathematical models using the adult mathematical phantom have been formulated for a variety of exposures both external and internal. Though the fifteen year-old mathematical phantom lends itself to similar applications, the "real world" exposure situation chosen is one of the administration of a radiopharmaceutical to an "average" fifteen year-old human. The method used has been that followed in the MIRD calculations for absorbed dose estimates to the "average" adult from biologically distributed radionuclides.³⁰ Because of its widespread use in Nuclear Medicine, technetium-99m has been chosen as a representative radionuclide.³¹ The administration of ^{99m}Tc is studied in the form of two different radiopharmaceuticals, sulfur-colloid and DMSA (2, 3-dimercaptosuccinic acid). ^{99m}Tc sulfur-colloid is used primarily in scans of the liver,

whereas DMSA is used for renal studies. The details of the modeling will be discussed for ^{99m}Tc sulfur-colloid. Any assumptions or methods used to obtain the results for DMSA which are different from those for sulfur-colloid are presented in Appendix B.

Absorbed Dose

The purpose of the modeling process is to calculate the absorbed dose to certain organs resulting from the exposure situation. The calculation of absorbed dose used here is based on the approach outlined by Loevinger and Berman in MIRD Pamphlet Number 1.³² The basic equation is

$$\bar{D}(v \leftarrow r) = \frac{\tilde{A}_r}{M_v} \sum_i \Delta_i \phi_i(v \leftarrow r) \quad \text{rads} \quad (2)$$

where

$\bar{D}(v \leftarrow r)$ = the mean dose to a target organ r from a source region v (rads),

\tilde{A}_r = the cumulated activity in the source region r ($\mu\text{Ci-h}$),

M_v = the mass of the target organ v (grams),

Δ_i = the equilibrium dose constant for the i^{th} type of radiation ($\text{g-rad}/\mu\text{Ci-h}$),

and

$\phi_i(v \leftarrow r)$ = the absorbed fraction of energy in the target organ from the source region v for the i^{th} type of radiation.

The mass of the target organ is merely the mass of the fifteen year-old organ in question as previously given in Chapter I. The methods used to calculate the other values needed in equation (2) are discussed later in this chapter. Once the values of $\bar{D}(v \leftarrow r)$ are calculated for

each source organ in the biological distribution, the mean dose to a target organ can be obtained by summing the values of $D(v \leftarrow r)$ over the source organs.

Decay Scheme Data

The decay scheme data for ^{99m}Tc are taken from the most recent calculations performed in connection with the MIRD Committee. The data in Figure 11 are published in the MIRD Pamphlet Number 10.⁵³ The data have also been presented in calculations using the one year-old and five year-old phantoms.¹⁸ As discussed in the MIRD Pamphlet Number 9,³³ the approach used in the Monte Carlo calculations leads to the calculation of the absorbed fraction for the complete ^{99m}Tc spectrum instead of each ith type of radiation.³³ Therefore, computing "effective absorbed fractions," ϕ_i , changes the term

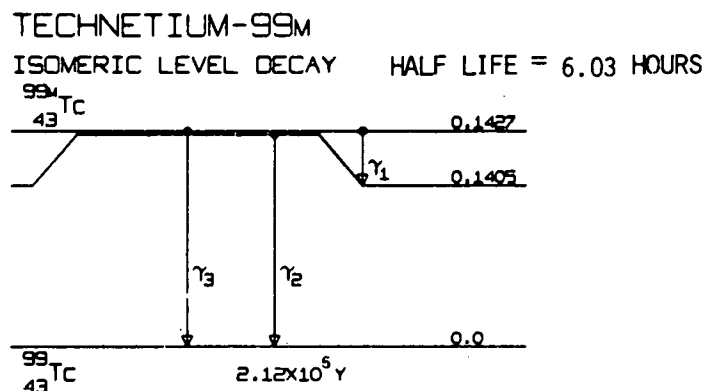
$$\sum_i \Delta_i \phi_i \quad \text{to the equivalent form} \quad \bar{\phi} \sum_i \Delta_i \quad (3)$$

It is evident that a summation of the Δ_i terms of Figure 11 yields a value

$$\sum_i \Delta_i = 0.2660 \quad (\text{g-rad}/\mu\text{Ci-h}) \quad (4)$$

Biological Model

The biological model for the radiopharmaceuticals is a result of unpublished work of Dr. E. M. Smith and has been used in calculations for the one year-old and five year-old phantoms.¹⁸ Numerical values for the model are presented in Table III for both ^{99m}Tc sulfur-colloid and ^{99m}Tc DMSA. The assumptions involved in deriving the values for the sulfur-colloid are as follows:



RADIATION		MEAN NUMBER/ DISINTE- GRATION	MEAN ENERGY/ PAR- TICLE	EQUI- LIBRIUM DOSE CONSTANT	DOSE CONSTANT FOR PENETRATING RADIATION
		N(I)	E(I) (MEV/ PAR- TICLE)	$\Delta(I)$ (G-RAD/ MICROCI- HOUR)	$\Delta(j)$ (G-RAD/ MICROCI- HOUR)
M INT CON	GAMMA	1	0.0000	0.0021	0.0000
	ELECT		0.9860	0.0016	0.0035
	GAMMA	2	0.8787	0.1405	0.2630
K INT CON	ELECT		0.0913	0.1194	0.0232
L INT CON	ELECT		0.0118	0.1377	0.0034
M INT CON	ELECT		0.0039	0.1400	0.0011
	GAMMA	3	0.0003	0.1426	0.0001
	ELECT		0.0088	0.1215	0.0022
L INT CON	ELECT		0.0035	0.1398	0.0010
M INT CON	ELECT		0.0011	0.1422	0.0003
K ALPHA-1	X-RAY		0.0441	0.0183	0.0017
K ALPHA-2	X-RAY		0.0221	0.0182	0.0008
K BETA-1	X-RAY		0.0105	0.0206	0.0004
KLL AUGER	ELECT		0.0152	0.0154	0.0005
KLX AUGER	ELECT		0.0055	0.0178	0.0002
LMM AUGER	ELECT		0.1093	0.0019	0.0004
MXY AUGER	ELECT		1.2359	0.0004	0.0011
				$\Sigma \Delta$	0.2660

FIGURE 11. ISOMERIC LEVEL DECAY OF ^{99m}Tc , DECAY DATA AND EQUILIBRIUM DOSE CONSTANTS.

- 1) the administered activity is instantaneously taken up by the organs and uniformly distributed in the organs,
- 2) the biological clearance of the material is much longer than the physical half-life of ^{99m}Tc , i.e. $T_{\text{eff}} = T_{1/2} \text{ phy}$,
- 3) the fraction of administered activity in the total body is assumed to be uniformly distributed in all tissues. This assumption will introduce an error of less than 5% in the total body dose.¹⁸

A more detailed presentation of the derivation of the following equations is presented in Appendix C. The basic equation for the cumulated activity is

$$\tilde{A}_r = \tilde{A}_{r_h}(\infty) = A_0 \sum_j \frac{q_{r_h^j}}{\lambda + \lambda_j} \quad (5)$$

where

$\tilde{A}_{r_h}(\infty)$ = the cumulated activity in the source region r_h over an infinite period ($\mu\text{Ci-h}$)

A_0 = the administered activity (μCi)

$q_{r_h^j}$ = the initial value of the j^{th} exponential component of the fraction of the administered substance as the labeled radiopharmaceutical that appears in the source region r_h .

λ_j = the biological disappearance constant of the j^{th} exponential component (1/h).

λ = the physical decay constant of the radionuclide (1/h).

Assuming A_0 equals 1 μCi and dividing both sides of equation (5) by A_0 one obtains the mean dose in units of rads per μCi administered activity, which is a more useful estimation of dose. With the above assumptions, the equation for a cumulated activity is

$$\tilde{A}_r' = \frac{q_r}{\lambda} \mu\text{Ci-h}/\mu\text{Ci administered} \quad (6)$$

where

q_r = the initial fraction of administered radiopharmaceutical in the source region r

λ = the physical decay constant for ^{99m}Tc .

Values for \tilde{A}_r' are given in Table IV for both radiopharmaceuticals. Substituting these results and the results from the decay scheme data into equation (2) gives the equation for dose

$$\bar{D}'(v \leftarrow r) = \frac{\tilde{A}_r'}{M_V} \bar{\phi}(v \leftarrow r) \sum_i \Delta_i \text{ rads}/\mu\text{Ci administered} \quad (7)$$

Monte Carlo Simulation

The only values in equation (7) that remain unassigned are the "effective absorbed fractions", $\bar{D}'(v \leftarrow r)$. At the heart of the calculation of such values must lie a model for simulating the transport of photons through the phantom. In 1966, "OGRE, A General-Purpose Monte Carlo Gamma-Ray Transport Code System" was developed at the Oak Ridge National Laboratory. This code has been used in studies of the transport of photons through different medium and geometries³⁴. Since that time, the code has been adapted to the geometry of the adult phantom to form a new code "ALGAM" which is used to calculate estimates of internal dose from gamma-ray sources.³⁵ A similar code using the geometry of the one year-old and five year-old phantoms has been used in estimates of dose from pediatric exposures with ^{99m}Tc .¹⁸ A detailed description of the OGRE code has been published.³⁴ However, a summary

TABLE IV
 CUMULATED ACTIVITY FOR ^{99m}Tc -SULFUR COLLOID AND ^{99m}Tc -DMSA

Source Organ	\tilde{A}_T ($\mu\text{Ci-h}/\mu\text{Ci Admin.}$)	
	Sulfur Colloid	DMSA
Bladder	-	0.220
Kidneys	-	5.190
Liver	7.360	0.387
Spleen	0.606	0.043
Red Marrow	0.433	-
Total Body	0.260	2.860

of those details which apply to a phantom geometry is found in Appendix D.

A Monte Carlo code, GAM-15, was developed using OGRE and the geometry of the fifteen year-old mathematical phantom in the same manner in which ALGAM was developed for the adult. The code is designed so that an operator familiar with the use of ALGAM can work easily with GAM-15. GAM-15 was designed to run on the Virginia Polytechnic Institute and State University's IBM 370/155 computers using a Fortran-H compiler.

The main purpose of GAM-15 is to calculate the fraction of photon energy from a particular source region that is deposited in a particular target region for any number of source photons. The entire code can be broken into three basic packages: (1) the source routines, (2) the geometry of the medium, and (3) the transport code. The transport code has been adopted in its entirety from OGRE.³⁴ The source routines and the geometry, however, are specific for the fifteen year-old and the exposure situation being modeled.

The purpose of the source routine package is to model a particular organ in the body which contains a radioactive source. Within the geometrical constraints of that particular organ, the program chooses randomly an initial X, Y, and Z coordinate for the location (starting coordinates) of the first photon history. Then the program chooses randomly three starting direction cosines for the photon. In accordance with the decay data for a particular radionuclide, the source routine assigns to the photon an initial energy characteristic of the energy spectrum for that radionuclide. In this example, the

energy spectrum used simulated the spectrum of ^{99m}Tc . The final task of the source routine is to assign to the source photon a statistical weight of 1.0 which is its probability of existence.

This information is passed into the transport part of the code. The transport section assigns to the photon a particular flight distance. Combining this distance with the above information, the coordinate position for a potential photon interaction is determined in terms of X' , Y' , and Z' . At this point the geometry package is used to determine the organ or region in which the photon lies. Once this medium is known, the total mass attenuation coefficient is used in a game of chance. If the result is not favorable, there is no interaction, and the photon continues in the same direction with the same energy. However, if the result is favorable the site is chosen as an interaction site. In this case, the program considers several possible interactions; (1) Compton scattering, (2) photoelectric effect, and (3) pair production. The energy deposition for this interaction is calculated and recorded in a bookkeeping system that keeps track of the energy deposited in each organ. If by chance the interaction site is in a region of bone, a special subroutine is used to calculate the amount of energy deposited to the red marrow, the yellow marrow, and the remaining portion of the bone.

In addition to experiencing a reduction in energy, the photon experiences a reduction in statistical weight. The history might be terminated here if it escapes from the phantom geometry, if its energy falls below 5 keV, or if its weight falls below 10^{-5} . If the history is not terminated, a new potential interaction site is determined, the

location in the phantom is determined, and the game begins again. This process is repeated until the photon is terminated for one of the three possible reasons. The path that the photon has traveled, the interactions encountered and the energy that it has deposited until its death is considered to be its history. When the first photon is terminated, the bookkeeping system has recorded its history and the program reinitializes parameters and a new source photon is born. GAM-15 repeats this process until the histories of 60,000 source photons are recorded.

After the required number of histories are recorded, GAM-15 estimates the average energy deposited in each organ per source photon emitted. Thus the value of absorbed fraction for each organ is calculated. In addition to the absorbed fractions, other values for each organ are calculated by the code. The coefficient of variation, the standard deviation and the number of photons that have an interaction are all used to determine the accuracy of the absorbed fraction for each organ. This is discussed in more detail in Appendix D. A sample output for GAM-15 is shown in Figure 12.

Tables V and VI give the values for $\bar{\phi}(v \leftarrow r)$ necessary for both ^{99m}Tc sulfur-colloid and ^{99m}Tc DMSA as calculated by GAM-15. Using the same computer and the same initial random number, the results should be identical. Using a different random number generator the values for $\bar{\phi}(v \leftarrow r)$ should be nearly the same. It is important to note that when the value of the coefficient of variation exceeds 50%, the estimate may be in error by a factor of 2 to 15.¹⁶

UNIFORM SOURCE IN THE FLAPPER FOR 99M-Tc 50,000 PHOTON HISTORIES
 NO. OF PHOTONS INITIAL ENERGY CUT-OFF ENERGY TOTAL NO. OF COLLISIONS
 60000 0.140 MEV 0.004 MEV 342053

DATE RUN, 11/06/75

ENERGY DISTRIBUTION
 EZERO PROB COUNT
 0.1405 0.9195000 55292
 0.0183 0.5656000 2657
 0.0182 0.5887000 1394
 0.0206 0.5597000 644
 0.1426 1.0000000 13

MEDIUM TOTAL XSECT SCAT PROB PAIR PROB
 1 0.1631E 03 0.1523E-02 0.0
 2 0.7384E 02 0.2923E-02 0.0
 3 0.2438E 02 0.2648E-02 0.0
 4 0.0 0.0 0.0

TERMINATION

1. ENERGY 3. WEIGHT 9136.
 3. ESCAPE 50864. 4. ABSORBED 0.

STANDARD REFERENCE MAN ORGANS

ORGAN	RADS/PHOTON	STD. DEV.	COEFF. VAR.	COLLISIONS	MASS	F (G-RADS)	VAR. OF F	ABSD. ERAC
1 LEFT ADRENAL	3.802E-16	3.302E-16	1.000E-00	2	4.559E 00	1.733E-15	3.004E-30	0.9378E-06
2 RIGHT ADRENAL	1.941E-15	1.187E-15	5.117E-01	4	4.559E 00	8.849E-15	2.930E-29	0.4777E-05
3 ADRENALS	1.160E-15	6.233E-16	5.371E-01	6	9.119E 00	1.053E-14	3.230E-29	0.5115E-05
4 BLADDER	6.397E-13	1.212E-14	1.895E-02	6530	3.447E 01	2.205E-11	1.746E-25	0.1066E-01
5 CONTENTS	1.111E-12	7.586E-15	7.178E-03	47210	1.531E 02	1.704E-10	1.455E-24	0.8235E-01
5 BRAIN	5.717E-18	5.717E-18	1.000E 00	1	1.344E 03	7.635E-15	5.906E-29	0.3715E-05
7 G.I. STOMACH	3.051E-15	3.874E-16	1.270E-01	214	1.163E 02	3.553E-13	2.029E-27	0.1715E-03
8 CONTENTS	2.773E-15	3.400E-16	1.226E-01	291	1.904E 02	5.279E-13	4.190E-27	0.2552E-03
9 G.I. U.L.I.	1.946E-14	9.227E-16	4.740E-02	1295	1.463E 02	2.847E-12	1.822E-26	0.1276E-02
10 CONTENTS	1.981E-14	9.540E-16	4.821E-02	1382	1.539E 02	3.043E-12	2.160E-26	0.1473E-02
11 G.I. L.L.I.	6.297E-14	2.000E-15	3.176E-02	2589	1.111E 02	6.933E-12	4.940E-26	0.3382E-02
12 CONTENTS	5.034E-14	1.913E-15	3.756E-02	1790	9.460E 01	4.750E-12	3.273E-26	0.2504E-02
13 SM.INT.+CONTS	2.017E-14	5.059E-16	2.508E-02	7228	7.427E 02	1.493E-11	1.412E-25	0.7242E-02
14 GENITALIA	4.184E-14	1.551E-15	3.706E-02	2086	1.517E 02	6.359E-12	5.537E-26	0.3069E-02
15 HEART	1.982E-16	6.733E-17	3.395E-01	34	2.379E 02	4.714E-14	2.566E-28	0.2281E-04
16 LEFT KIDNEY	2.224E-15	3.329E-16	1.497E-01	152	1.165E 02	2.592E-13	1.505E-27	0.1253E-03
17 RIGHT KIDNEY	2.552E-15	3.179E-16	1.246E-01	197	1.165E 02	2.974E-13	1.373E-27	0.1437E-03
18 KIDNEYS	2.386E-15	2.301E-16	9.635E-02	349	2.331E 02	5.565E-13	2.875E-27	0.2650E-03
19 LIVER	1.397E-15	9.950E-17	7.121E-02	1221	1.267E 03	1.771E-12	1.590E-26	0.8560E-03
20 LEFT LUNG	1.185E-16	3.638E-17	3.231E-01	38	3.251E 02	3.882E-14	1.557E-28	0.1867E-04
21 RIGHT LUNG	4.634E-16	1.118E-16	2.415E-01	62	3.251E 02	1.507E-13	1.322E-27	0.7282E-04
22 LUNGS	2.911E-16	5.512E-17	2.031E-01	100	6.502E 02	1.893E-13	1.477E-27	0.9148E-04

FIGURE 12. A SAMPLE OUTPUT OF GAM-15.

23	RM UP.L.ARM	1.572E-16	1.087E-16	6.888E-01	9	1.425F 01	2.248E-15	2.399F-30	0.1067F-05
24	RM LO.L.ARM	8.375F-14	2.299F-15	2.745E-02	6849	6.090F 01	5.101F-12	1.960F-26	0.2465F-02
25	RM UP.R.ARM	2.792F-16	1.486E-16	5.321E-01	11	1.425F 01	7.979F-15	4.482F-30	0.1923F-05
26	RM LO.R.ARM	1.139F-14	7.224F-16	6.339F-02	890	6.090F 01	6.939E-13	1.935F-27	0.3354F-03
27	RM CLAVICLES	9.504E-19	9.504E-19	1.000F 00	4	9.500E 00	9.029E-18	8.152F-35	0.4364F-08
28	RM UP.L.LEG	0.0			0	7.740F 01	0.0		0.0
29	RM LO.L.LEG	0.0			0	9.205F 00	0.0		0.0
30	RM UP.R.LEG	1.279E-14	3.937E-16	3.079F-02	5692	7.240F 01	9.259F-13	8.124F-28	0.4475F-03
31	RM LO.R.LEG	1.874E-16	4.603E-17	2.456E-01	79	9.205E 00	1.725E-15	1.795F-31	0.6338F-06
32	RM PFLVIS	4.610E-14	7.550E-16	1.638F-02	12883	2.280E 02	1.051E-11	2.963E-26	0.5090F-02
33	RM RIBS	6.854F-16	7.514E-17	1.056E-01	244	7.600E 01	5.709F-14	3.761F-29	0.2518F-04
34	RM SCAPULAE	1.403E-16	5.374E-17	3.830F-01	10	7.800E 01	5.332E-15	4.170E-30	0.2577F-05
35	RM CRANIUM	0.0			0	9.550E 01	0.0		0.0
36	RM MANDIBLE	0.0			0	9.500F 00	0.0		0.0
37	RM LOW.SPINE	1.160E-14	6.998E-16	6.032E-02	1499	7.290F 01	8.458E-13	2.603F-27	0.4098F-03
38	RM MID.SPINE	6.489E-16	9.118F-17	1.405F-01	263	9.420F 01	6.113F-14	7.378E-29	0.2955F-04
39	RM UPP.SPINE	1.601F-19	1.601F-19	1.000E 00	2	2.270F 01	3.635E-18	1.321F-35	0.1757F-08
40	RM MID.REGION	5.065F-16	4.581E-17	5.038E-02	541	2.462E 02	1.248E-13	1.272F-28	0.6032F-04
41	RM LOW.REGION	3.084F-14	3.996E-16	1.296F-02	27892	5.359E 02	1.807F-11	5.483F-26	0.8734F-02
42	RM HEAD	3.088E-20	3.088E-20	1.000F 00	7	1.177F 02	3.635E-18	1.321F-35	0.1757F-08
43	RED MARROW	1.916E-14	2.469E-16	1.289E-02	28435	9.498E 02	1.820E-11	5.498E-26	0.8755F-02
44	YM UP.L.ARM	1.578E-16	1.087E-16	6.888E-01	9	1.250E 00	1.972F-16	1.846F-32	0.9533F-07
45	YM LO.L.ARM	6.584E-14	1.807E-15	2.745E-02	6849	9.755F 01	6.449E-12	3.134F-26	0.3117F-02
46	YM UP.R.ARM	2.792E-16	1.486E-16	5.321F-01	11	1.250F 00	3.490F-16	3.449F-32	0.1687F-06
47	YM LO.R.ARM	8.958E-15	5.679E-16	6.339F-02	890	9.795F 01	8.775E-13	3.094F-27	0.4241F-02
48	YM CLAVICLES	9.504F-19	9.504E-19	1.000E 00	4	1.660E 01	1.578E-17	2.489F-34	0.7625F-08
49	YM UP.L.LEG	0.0			0	2.415E 01	0.0		0.0
50	YM LO.L.LEG	0.0			0	1.135F 02	0.0		0.0
51	YM UP.R.LEG	3.059E-14	9.418F-16	3.079F-02	5692	2.415E 01	7.388F-13	5.173F-29	0.3571F-03
52	YM UPP.SPINE	1.864E-16	4.578E-17	2.456E-01	79	1.135E 02	2.117F-14	2.703F-29	0.1023F-04
53	YM PELVIS	4.610E-14	7.550E-16	1.638F-02	12883	3.633F 02	1.675E-11	7.523F-26	0.8095F-02
54	YM RIBS	4.995E-16	5.475E-17	1.056E-01	244	2.131F 02	1.064E-13	1.361F-28	0.5144F-04
55	YM SCAPULAE	1.403F-16	5.374E-17	3.830E-01	10	4.040E 01	5.669E-15	4.713F-30	0.2740F-05
56	YM CRANIUM	0.0			0	1.089E 02	0.0		0.0
57	YM MANDIBLE	0.0			0	1.010E 01	0.0		0.0
58	YM LOW.SPINE	1.160E-14	6.998E-16	6.032E-02	1499	1.051E 02	1.219E-12	5.409E-27	0.5894F-02
59	YM MID.SPINE	6.489E-16	9.118F-17	1.405E-01	263	1.361F 02	8.832E-14	1.540E-28	0.4265E-04
60	YM UPP.SPINE	1.601E-19	1.601E-19	1.000E 00	2	3.280F 01	5.252E-18	2.759F-35	0.2539F-08
61	YM MID.REGION	4.610E-16	4.344E-17	8.834F-02	541	4.087E 02	2.010E-13	3.152E-28	0.9714E-04
62	YM LOW.REGION	2.772F-14	3.628F-16	1.309E-02	27892	9.397F 02	2.605E-11	1.162F-25	0.1259F-01
63	YM HEAD	3.460E-20	3.460E-20	1.000E 00	7	1.518E 02	5.252F-13	2.759F-35	0.2539F-08
64	YELLOW MARROW	1.750E-14	2.276E-16	1.301E-02	28435	1.500F 03	2.625F-11	1.166F-25	0.1269F-01
65	SEPTUM	0.0			0	1.424E 01	0.0		0.0
66	NARFS	0.0			0	9.495E 00	0.0		0.0
67	NASAL REGION	0.0			0	2.374F 01	0.0		0.0
68	LEFT OVARY	5.94CF-14	1.064E-14	1.792E-01	70	2.595E 00	1.541E-13	7.626F-28	0.7449F-04
69	RIGHT OVARY	3.385F-14	7.913E-15	2.335F-01	41	2.555E 00	8.794E-14	4.215F-28	0.4251F-04
70	OVARIES	4.665F-14	6.657F-15	1.427E-01	111	5.189E 00	2.421E-13	1.193F-27	0.1170F-02
71	PANCREAS	2.754F-15	5.662F-16	2.056F-01	93	5.638E 01	1.553E-13	1.019F-27	0.7505F-04
72	LEFT ARM BONE	2.773E-14	7.609E-16	2.743F-02	6858	5.952E 02	1.651E-11	2.051F-25	0.7979F-02
73	RT. ARM BONE	3.804E-15	2.399F-16	6.306F-02	901	5.952E 02	2.264E-12	2.039F-26	0.1094E-02
74	CLAVICLES	9.504E-19	9.504E-19	1.000E 00	4	6.799E 01	6.462E-17	4.176F-33	0.3123F-07
75	LEFT LEG BONE	0.0			0	1.658F 03	0.0		0.0
76	RT. LEG BONE	8.614F-15	2.637E-16	3.061F-02	5771	1.658E 03	1.428E-11	1.911F-25	0.6902F-02
77	PELVIS	4.611E-14	7.549E-16	1.637F-02	12883	7.550F 02	3.481F-11	3.249E-25	0.1683F-01
78	RIBS	5.483E-16	6.011E-17	1.056E-01	244	8.639E 02	4.737E-13	2.697E-27	0.2250F-02
79	SCAPULAE	1.403E-16	5.374E-17	3.830E-01	10	2.529F 02	3.549E-14	1.847F-28	0.1715F-04
80	SKULL	0.0			0	1.183F 03	0.0		0.0

FIGURE 12 (CONTINUED). A SAMPLE OUTPUT OF GAM-15.

81 SPINE	3.095E-15	1.744E-16	5.627E-02	1764	1.104E 03	3.421E-12	3.705E-26	0.1653E-02
82 SKELETON	8.215E-15	1.011E-16	1.230E-02	28435	9.733E 03	7.178E-11	7.801E-25	0.3469E-01
83 TRUNK SKIN	7.190E-15	2.067E-16	2.874E-02	2626	1.154E 03	8.295E-12	5.695E-26	0.4009E-02
84 LEG SKIN	3.405E-15	1.407E-16	4.132E-02	1392	1.044E 03	3.554E-12	2.157E-26	0.1718E-02
85 HEAD SKIN	0.0			0	2.481E 02	0.0		0.0
86 TOTAL SKIN	4.844E-15	1.143E-16	2.359E-02	4018	2.446E 03	1.185E-11	7.813E-26	0.5726E-02
87 SPLEEN	1.762E-15	3.166E-16	1.796E-01	130	1.415E 02	2.494E-13	2.008E-27	0.1206E-03
88 LEFT TESTE	5.462E-14	7.236E-15	1.325E-01	143	7.779E 00	4.249E-13	3.168E-27	0.2054E-03
89 RIGHT TESTE	6.059E-14	7.239E-15	1.195E-01	157	7.779E 00	4.713E-13	3.171E-27	0.2278E-03
90 TESTES	5.760E-14	5.193E-15	9.015E-02	300	1.556E 01	8.962E-13	6.527E-27	0.4322E-03
91 THYMUS	4.120E-17	4.120E-17	1.000E 03	1	2.698E 01	1.112E-15	1.236E-30	0.5375E-06
92 THYROID	0.0			0	1.319E 01	0.0		0.0
93 TRUNK TISSUE	2.311E-14	9.984E-17	4.320E-03	204761	2.462E 04	5.691E-10	6.044E-24	0.2751E 00
94 LEG TISSUE	5.190E-15	7.049E-17	1.358E-02	30886	1.318E 04	6.340E-11	8.631E-25	0.3306E-01
95 HEAD TISSUE	3.510E-18	2.992E-18	8.524E-01	5	2.073E 03	7.277E-15	3.947E-29	0.3517E-05
96 TOTAL TISSUE	1.599E-14	6.477E-17	4.052E-03	235652	3.589E 04	6.375E-10	6.671E-24	0.3081E 00
97 UTERUS	1.529E-13	6.558E-15	4.290E-02	1391	2.881E 01	4.404E-12	3.569E-26	0.2128E-02
98 TRUNK	2.494E-14	8.698E-17	3.487E-03	296082	3.426E 04	8.546E-10	8.881E-24	0.4151E 00
99 LEGS	6.060E-15	7.385E-17	1.219E-02	45963	1.753E 04	1.062E-10	1.675E-24	0.5134E-01
100 HEAD	2.972E-18	2.134E-18	7.181E-01	8	5.042E 03	1.499E-14	1.158E-28	0.7244E-05
101 TOTAL BODY	1.686E-14	5.504E-17	3.264E-03	342053	5.698E 04	9.609E-10	9.837E-24	0.4644E 00

FIGURE 12 (CONTINUED). A SAMPLE OUTPUT OF GAM-15.

TABLE V

ABSORBED FRACTIONS FOR THE PHOTON SPECTRUM OF ^{99m}Tc FOR THE FIFTEEN YEAR-OLD HUMAN PHANTOM

Target Organs	Source Organs					
	Bladder Contents	Kidneys	Liver	Spleen	Red Marrow	Total Body
Adrenals	5.115E-06*	4.768E-04	1.305E-04	5.369E-04	7.754E-05	5.643E-05
Bladder Wall	1.066E-02	4.314E-04	3.505E-05	2.648E-05	1.226E-04	2.919E-04
Brain	3.715E-06*	1.584E-05	4.132E-05	6.930E-05	6.966E-03	6.229E-03
Stomach	1.715E-04	1.610E-03	1.293E-03	4.419E-03	4.648E-04	9.099E-04
S.I. (wall & contents)	7.242E-03	1.085E-02	1.022E-02	6.426E-03	6.327E-03	7.042E-03
U.L.I. (wall	1.376E-03	1.679E-03	2.269E-03	9.665E-04	8.969E-04	1.276E-03
L.L.I. (wall	3.382E-03	3.389E-04	1.125E-04	3.240E-04	1.079E-03	1.009E-03
Heart	2.281E-05	8.656E-03	2.387E-03	1.767E-03	1.007E-03	1.811E-03
Kidneys	2.690E-04	6.534E-02	3.386E-03	1.133E-02	1.690E-03	1.549E-03
Liver	8.560E-04	1.866E-02	1.393E-01	9.188E-03	4.552E-03	9.238E-03
Lungs	9.148E-05	2.586E-03	5.887E-03	6.366E-03	3.509E-03	3.367E-03
Ovaries	1.170E-04	2.601E-05	2.577E-05	1.478E-05	4.922E-05	4.514E-05
Pancreas	7.505E-05	1.374E-03	1.210E-03	5.401E-02	3.963E-03	5.724E-04
Skeleton	3.469E-01	4.795E-02	3.898E-02	4.679E-02	1.366E-01	6.919E-02
Red Marrow	8.795E-03	1.039E-02	7.852E-03	9.077E-03	3.044E-02	1.277E-02
Yellow Marrow	1.269E-02	1.536E-02	1.149E-02	1.335E-02	4.102E-01	1.786E-01
Skin	5.726E-03	5.588E-03	5.146E-03	4.820E-03	6.341E-03	9.224E-03
Spleen	1.206E-04	7.522E-03	7.982E-04	7.493E-02	7.175E-04	1.043E-03
Testes	4.332E-04	4.068E-07*	5.647E-06*	1.445E-07*	1.801E-05	9.978E-04
Thymus	5.373E-07*	1.042E-05	6.295E-05	3.809E-05	1.091E-04	1.339E-04
Thyroid	0.0	5.136E-06*	0.0	1.897E-05	3.857E-05	1.055E-04
Uterus	2.128E-03	9.498E-05	5.636E-05	6.153E-05	1.745E-04	2.330E-04
Total Body	4.644E-01	3.968E-01	4.155E-01	4.302E-01	3.658E-01	3.459E-01

*The coefficient of variation for these values is greater than 50%.

TABLE VI
 ABSORBED DOSE TO SELECTED ORGANS FROM ^{99m}Tc -SULFUR COLLOID

Target Organ	Dose for Source Organs: $\bar{D}'(\lambda + r)$ rads/ μCi Admin.				Total Dose to Target: \bar{D}_v rads/ μCi Admin.
	Liver	Spleen	Red Marrow	Total Body	
Bladder	1.9907E-06	1.2383E-07	4.0966E-07	5.9566E-07	3.1098E-06
Heart	1.9643E-05	1.1973E-06	4.8753E-07	5.2648E-07	2.1854E-05
Kidneys	2.8433E-05	7.8350E-06	8.3505E-07	4.5958E-07	3.7568E-05
Liver	2.1524E-04	1.1690E-06	4.1380E-07	5.0426E-07	2.1733E-04
Lungs	1.7725E-05	1.5782E-06	6.2159E-07	3.5814E-07	2.0284E-05
Ovaries	9.7228E-06	4.5914E-07	1.0925E-06	6.0163E-07	1.1876E-05
Red Marrow	1.6181E-05	1.5402E-07	3.6905E-06	9.2966E-07	2.0955E-05
Spleen	1.0919E-05	8.5360E-05	5.8403E-07	5.0978E-07	9.7373E-05
Uterus	3.8299E-06	3.4427E-07	6.9762E-07	5.5933E-07	5.4311E-06
Total Body	1.4276E-05	1.2170E-06	7.3942E-07	4.1984E-07	1.6652E-05

Estimates of Absorbed Dose

With the results from the Monte Carlo calculations, the necessary values have been obtained to calculate $\bar{D}'(v \leftarrow r)$ for each target organ and each source organ. Target organs chosen were those with a coefficient of variation less than 50% for all of the source organs in the biological distribution for the radiopharmaceutical. The final estimate of dose for a particular organ is obtained by summing the results for each source organ.

$$\bar{D}_v = \sum_r \bar{D}'(v \leftarrow r) \quad \text{rads}/\mu\text{Ci administered.} \quad (8)$$

Table VII gives the estimates for the absorbed dose estimates resulting from both calculations; the administration of ^{99m}Tc sulfur-colloid and the administration of ^{99m}Tc DMSA.

TABLE VII
 ABSORBED DOSE TO SELECTED ORGANS FROM ^{99m}Tc-DMSA

Target Organ	Dose from Source Organs: $\bar{D}'(v + r)$ rads/ μ Ci Admin.					Total Dose to Target: D_v rads/ μ Ci Admin.
	Bladder	Kidneys	Liver	Spleen	Total Body	
Bladder	1.8098E-05	1.7278E-06	1.0467E-07	8.7367E-09	6.4423E-06	2.6382E-05
Heart	5.6109E-09	5.0231E-05	1.0329E-06	8.4956E-08	5.7912E-06	5.7146E-05
Kidneys	6.7533E-08	3.8698E-04	1.4953E-06	5.5595E-07	5.0554E-06	3.9415E-04
Liver	1.7971E-07	2.0332E-05	1.1318E-05	8.2946E-08	5.5469E-06	3.7460E-05
Lungs	8.2335E-09	5.4907E-06	9.3205E-07	1.1199E-07	3.9395E-06	1.0482E-05
Ovaries	1.3195E-06	6.9200E-06	5.1124E-07	3.2579E-08	6.6180E-06	1.5401E-05
Red Marrow	5.4177E-07	1.5099E-05	8.5034E-07	1.0929E-08	1.0226E-05	2.6728E-05
Spleen	4.9876E-08	7.3388E-05	5.7415E-07	6.0569E-06	5.6076E-05	8.5676E-05
Uterus	4.3225E-06	4.5513E-06	2.0138E-07	2.4428E-08	6.1526E-06	1.5252E-05
Total Body	4.7695E-07	9.6139E-06	7.4066E-07	8.6357E-08	4.6182E-06	1.5546E-05

CHAPTER IV

CONCLUSIONS AND RECOMMENDATIONS

It is normal when drawing conclusions, to approach them from a comparative analysis. Either one compares the results of the research with the actual "real world" situation or with previous work that has relevance. Comparisons of this nature are not possible using the results of this research. At present there are no means to measure directly the radiation absorbed in living human tissue. Thus, it is impossible to construct a table of absorbed doses describing the real situation. Results of a similar experiment for an average fifteen year-old human are also not available. Most studies of radiation exposure have been performed with the concern of dose to the average adult.

The "reliability" of the values in Tables V and VI is determined not by a comparison, but by the reliability of the methods and models used in their determination. The biological model, the decay scheme, and the Monte Carlo calculation were all adopted in total. The physical decay scheme is well established and introduces little uncertainty into the results. The assumptions used in the biological model are not as well established and must be taken into consideration when applying the results in real situations. However, the biological model is based on careful consideration of the available data by a panel of experts; i.e. the MIRD Committee. The Monte Carlo calculations have inherent statistical uncertainties. The coefficients of variation are designed to be a measure of this uncertainty and with proper use one can obtain reliable data from this method. The term

"reliable" is indeed qualitative, but lack of experimental data dictates the subjective rather than the objective nature of absorbed dose estimates.

The purpose of the research was not to improve the reliability of the methods and models above, but to develop the model of the fifteen year-old. The limitations of the idealization are obvious. The most serious of these are the model of the skeletal system and the static nature of some of the organ designs. A better model for the bone and marrow is needed but lack of anatomical data for younger age groups prevents the design of such a model. A dynamic design for organs like the bladder could introduce significant differences in dose estimates. Studies concerned with the dose to a dynamic bladder are being performed for the adult and some adaptations are needed for the fifteen year-old design.³⁶

As new studies allow more conclusive anatomical data to be obtained, the phantom should be updated. Better mathematical representations for the organs are being developed at ORNL as well as at other laboratories. As these new idealizations evolve, they should be incorporated into the design of the mathematical phantom. As a confirmation for the existence of a phantom based on anatomical data, similar estimates should be calculated using the similitude phantom representing the average fifteen year-old. Although one would expect there to be large differences, there is much to be gained by a comparison of absorbed doses. To provide a check on the computational methods using the phantom construct, it would be useful to design a physical phantom that corresponds to the mathematical phantom and generate similar data obtained experimentally.

No other anatomically based idealization of an "average" fifteen year-old human is in existence for purposes of estimating absorbed dose. The phantom is a marked improvement over the use of a "small adult" for setting standards of exposure to radiation. There is merit also in the fact that this development brings estimates of dose for the fifteen year-old to the same level of sophistication accepted by the ICRP for present estimates of dose for the average adult. Therefore the fifteen year-old equivalent mathematical phantom should stand not as a final model, but as a foundation on which to improve estimates of absorbed dose for groups other than the adult.

BIBLIOGRAPHY

1. Myers, W. G., Wagner, H. N., Jr. (1975). "How It Began," Nuclear Medicine, H. N. Wagner, Jr., Ed., H. P. Publishing Co., Inc., pp. 3-16.
2. Schubert, J., Lapp, R. E. (1957). Radiation: What It Is and How It Affects You, Viking Press, p. 112.
3. Hevesy, G. (1948). Radioactive Indicators, Interscience Pub., Inc.
4. Lawrence, E. O. (1939). "The Medical Cyclotron at the William H. Crocker Radiation Laboratory," Science, 90: 407.
5. Joliot, F., Curie, I. (1934). "Artificial Production of a New Kind of Radioelement," Nature, 133: 201.
6. Chiewitz, O., Hevesy, G. (1935). "Radioactive Indicators in the Study of Phosphorous Metabolism in Rats," Nature, 136: 754.
7. Taylor, L. S. (1958). Health Physics, 1: 306.
8. Mulscheller, A. M. (1925). Am. Jour. Roentgenol. Radium Therapy Nuc. Med., 13: 65.
9. Snyder, W. S. (1967). "Internal Exposure," Principles of Radiation Protection, K. Z. Morgan, Ed., John Wiley and Sons, Inc., pp. 301-304.
10. Morgan, K. Z. (1967). "History of Damage and Protection From Ionizing Radiation," Principles of Radiation Protection, John Wiley and Sons, Inc., pp. 1-75.
11. Morgan, K. Z. (1967). "Maximum Permissible Exposure Levels. External and Internal," Principles of Radiation Protection, John Wiley and Sons, Inc., pp. 497-537.
12. Adelstein, S. J. (1975). "Radiation Risks," Nuclear Medicine, H. N. Wagner, Jr., Ed., H. P. Publishing Co., Inc., pp. 73-82.
13. Bland, W. H. (1971). Nuclear Medicine, McGraw-Hill Book Company, p. 156.
14. Snyder, W. S., Cook, M. J., Nasset, E. S., Karhausen, L., Howells, G. P., Tipton, I. H. (1975). Report of the Task Group on Reference Man, ICRP No. 23, Pergamon Press.
15. Fisher, H. L., Jr., Snyder, W. S. (1966). Oak Ridge National Laboratory Report, ORNL-4007.

16. Snyder, W. S., Ford, M. R., Warner, G. G., Watson, S. B. (1974). "A Tabulation of Dose Equivalent Per Microcurie-Day for Source and Target Organs of an Adult for Various Radionuclides," ORNL-5000.
17. Warner, G. G., Poston, J. W., Snyder, W. S. (1974). "Absorbed Dose in Male Humanoid Phantoms from External Sources of Photons as a Function of Age," Health Phys. Div. Ann. Prog. Report for Period Ending July 31, 1974, ORNL-4979, pp. 40-45.
18. Hwang, J. M. (1975). "Mathematical Descriptions of a One- and Five-Year Old Child for Use in Dosimetric Calculations," M.S. Thesis, The University of Tennessee.
19. Tipton, I. H., Snyder, W. S., Cook, M. J. (1966). "Elemental Composition of Standard Man," Health Phys. Div. Ann. Prog. Report for Period Ending July 31, 1966, ORNL-4007, p. 241.
20. Banley, W. (1956). "Growth Curves of Height and Weight by Age for Boys and Girls Scaled According to Physical Maturity," J. Pediatrics, 48: 187-194.
21. Boyd, E. (1933). "The Specific Gravity of the Human Body," Human Biology, 5: 646-672.
22. Bardeen, C. R. (1920). "The Height-Weight Index of Build in Relation to Linear and Volumetric Proportions and Surface-Area of the Body During Post-Natal Development," Contributions to Embryology, 46: 483-552.
23. Pryor, H. B. (1966). "Charts of Normal Body Measurements and Revised Width-Weight Tables in Graphic Form," J. Pediatrics, 68: 615-631.
24. Jackson, C. M. (1928). "Some Aspects of Form and Growth," Growth, W. J. Robbins, S. Brody, A. G. Hogan, C. M. Jackson, C. W. Greene, Authors, Yale University Press, pp. 111-140.
25. Ingalls, N. W. (1931). "Observations on Bone Weights," Am. J. Anat., 48: 45-98.
26. Shleien, B. (1973). A Review of Determinations of Radiation Dose to the Active Bone Marrow from Diagnostic X-Ray Examinations, DHEW and FDA 74-8007.
27. Mechanik, W. (1926). "Untersuchungenuber das Gewicht des Knochenmarkes des Menschen," (Investigations on the Weight of Bone Marrow of Man), Z. Anat. Entwickl, 79: 58-99.
28. Underhill, B. M. L. (1955). "Intestinal Length in Man," Brit. Med. J., Nov., pp. 1243-1246.

29. Garry, S. M. (1974). "Measurement of Absorbed Fractions for Photon Sources Distributed Uniformly in Various Organs of a Heterogeneous Phantom," M.S. Thesis, The University of Tennessee.
30. Snyder, W. S., Ford, M. R., Warner, G. G., Fisher, H. L., Jr. (1968); MIRD Pamphlet No. 5, J. Nucl. Med., 10, Suppl. No. 3.
31. Winchell, H. S. (1975). "Radiopharmaceuticals," Nuclear Medicine, H. N. Wagner, Jr., Ed., H. P. Publishing Co., Inc., pp. 61-72.
32. Loevinger, R., Berman, M. (1968). "A Schema for Absorbed Dose Calculation for Biologically-Distributed Radionuclides," MIRD Pamphlet No. 1, J. Nucl. Med., Suppl. No. 1.
33. Lathrop, K. A., et al., (1972). "Radiation Dose to Humans from ^{75}Se -L-Selenomethionine," J. Nuc. Med., Suppl. No. 6.
34. "OGRE, General-Purpose Monte Carlo Gamma-Ray Transport Code System," Radiation Shielding Information Center, ORNL, Oak Ridge, Tennessee, CCC-46.
35. Warner, G. G., Craig, A. M., Jr. (1968). Algam, A Computer Program for Estimating Internal Dose from Gamma-Ray Sources in a Man Phantom, ORNL-TM-2250.
36. Snyder, W. S., Poston, J. W., Warner, G. G., Owen, L. W. (1974). "Dose to a Dynamic Bladder for Administered Radionuclides," Health Phys. Div. Ann. Prog. Report for Period Ending July 31, 1974, ORNL-4979.
37. Personal communication of Dr. C. M. Smith to Dr. J. W. Poston (1975).
38. Grodstein, G. W. (1957). X-Ray Attenuation Coefficients for 10 keV to 100 MeV, National Bureau of Standards Circular 583.
39. McGinnis, R. T. (1959). Supplement to NBS Circular 583.
40. National Academy of Sciences - National Research Council (1964). Studies in Penetration of Charged Particles in Matter, Publication 1133, p. 266.
41. Boyd, E. (1952). An Introduction to Human Biology and Anatomy for First Year Medical Students, Child Research Council, Denver.
42. Altman, P. L., Dittmer, D. S. (1962). "Growth Including Reproduction and Morphological Development," Biological Handbook, (Federation of Am. Soc. Exptl. Biol., Washington).

43. White House Conference on Child Health and Protection called by President Herbert Hoover (1933). "Growth and Development of the Child, Part II. Anatomy and Physiology," Report of the Committee on Growth and Development, K. D. Blackfan, Chairman, The Century Company.
44. Scammon, R. E., Dunn, H. L. (1922). "Empirical Formulae for the Postnatal Growth of the Human Brain and Its Major Divisions," Proc. Soc. Exptl. Biol. Med., 20: 114-117.
45. Scammon, R. E. (1927). "The Developmental Anatomy of the Chest and the Thoracic Organs," The Normal Chest of the Adult and the Child, J. A. Myers, Ed., Williams and Wilkins, Co., pp. 300-335.
46. Krogman, W. M. (1941). "Growth of Man," Tabulae Biologicae, H. Denzer, V. J. Koningsberger, H. J. Vonk, Eds., Vol. 20: 1-963.
47. Stolpe, Y., King, L. R., White, H. (1967). "The Normal Range of Renal Size in Children," Invest. Urology, 4: 600-607.
48. Engel, S. (1947). The Child's Lung. Development Anatomy, Physiology and Pathology, Edward Arnold and Co.
49. Scammon, R. E. (1930). "The Growth of the Human Reproductive System," Second International Congress for Sex Research, London, 1930, A. W. Greenwood, Ed., pp. 118-123.
50. Spencer, R. P., Chandhuri, J. K. (1969). "Quantitative Estimates of Changes in Splenic Size During Life," Yale J. of Biol. and Med., 41: 333-339.
51. Kay, Chester, Abrahams, S., McClain, P. (1966). "The Weight of Normal Thyroid Glands in Children," Arch. Pathol., 82: 349-352.
52. Villforth, J. (1974). "Population Exposures from Medical Sources and Their Control," Proceedings of the Eighth Midyear Topical Symposium of the Health Physics Society, Knoxville, Tennessee, CONF-741018.
53. Dillman, L. T., Von der Lage, F. C. (1975). MIRD Pamphlet No. 10, J. Nucl. Med.

APPENDIX A

THE EQUATIONS DESCRIBING THE FIFTEEN YEAR-OLD EQUIVALENT MATHEMATICAL PHANTOM

The following set of equations formulate the mathematical construct used to represent an "average" fifteen year-old human. These equations have been coded into a fortran plotting routine used to display the boundary points of the organs described by the equations. The resulting plots are cross sectional views of the phantom and are presented as Figures 2 through 7 in Chapter II. The equations are cast in an X, Y, and Z coordinate system with the origin at the center of the base of the trunk section. Many of the organ pairs are symmetrical with respect to the Y axis. In this case one equation will be written using the conventional \pm sign, where the "plus" describes the organ to the reader's left of the Y axis and the "minus" describes the one to the reader's right.

Both the mass and the volume of the principal sections are given. However, only the volume is given for those organs within each section. The mass of these organs is obtained easily by multiplying the given volume by the proper density; 1.4862 g/cm³, 0.3 g/cm³ or 0.9889 g/cm³ for bone, lungs, or soft tissue respectively. The skin of the phantom is considered to be a layer of soft tissue 0.2 cm thick on all exterior surfaces of the phantom. The phantom has a mass of 57 kg and a total volume of 56,300 cm³. The equations will be given according to their location in one of the three principal sections. The axes are given in centimeters.

The head section is a right elliptical cylinder topped by a hemisphere (Figure 1, page 12) with a mass of 5042 g and a volume of 4655 cm³. The defining equations are

$$\left(\frac{X}{7}\right)^2 + \left(\frac{Y}{10}\right)^2 \leq 1, \quad 67.2 \leq Z \leq 82.7$$

and

$$\left(\frac{X}{7}\right)^2 + \left(\frac{Y}{10}\right)^2 + \left(\frac{Z - 82.7}{8.5}\right)^2 \leq 1, \quad 82.7 \leq Z \leq 91.2.$$

The skull (Figure 8, page 23) is the space between two ellipsoids and has a volume of 796 cm³. The defining equations are

$$\left(\frac{X}{6.8}\right)^2 + \left(\frac{Y}{9.8}\right)^2 + \left(\frac{Z - 82.7}{8.3}\right)^2 \leq 1$$

and

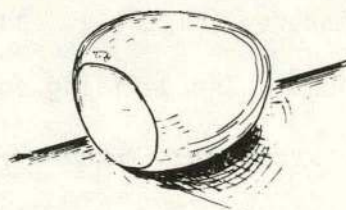
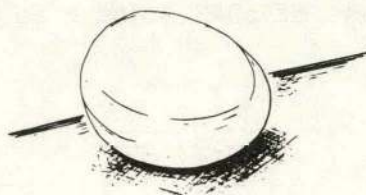
$$\left(\frac{X}{6.1}\right)^2 + \left(\frac{Y}{9.1}\right)^2 + \left(\frac{Z - 83.7}{6.54}\right)^2 \geq 1.$$

The brain (Figure A-1) is an ellipsoid cut by a plane on the bottom side having a total volume of 1367 cm³ as defined by

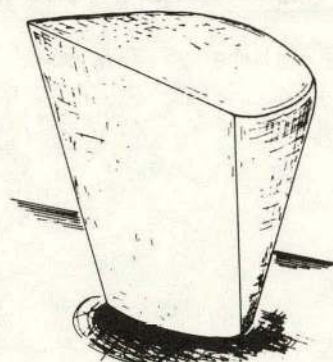
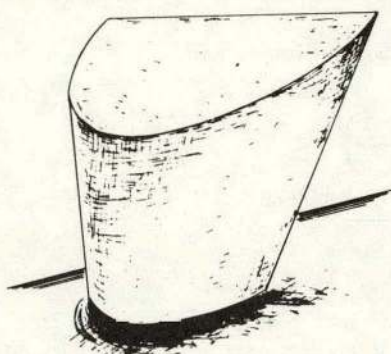
$$\left(\frac{X}{6.1}\right)^2 + \left(\frac{Y}{9.1}\right)^2 + \left(\frac{Z - 83.7}{6.54}\right)^2 \leq 1$$

and

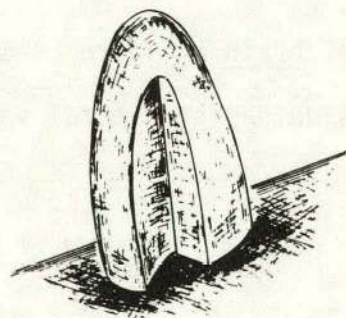
$$Z \geq 78.78.$$



HEART



LIVER



BRAIN

LUNG

FIGURE A-1. MATHEMATICAL MODELS FOR THE HEART, LIVER, BRAIN AND LUNGS.

The nasal region (Figure 10, page 31) is composed of three sections; two nares divided by a septum. The total volume is 24 cm^3 defined by

$$73.2 \leq Z \leq 76.7,$$

$$Y \geq -2.936,$$

and

$$(Y + 6.436)^2 + (Z - 73.2)^2 \leq (3.5)^2,$$

with the nares defined by

$$\pm .25 \leq X \leq \pm .375$$

and the septum is defined by

$$-.375 < X < .375.$$

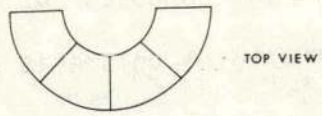
The lobes of the thyroid (Figure A-2) lie in the volume between two concentric cylinders with a total organ volume of 13 cm^3 as defined by

$$X^2 + (Y + 6)^2 \leq (1.927)^2,$$

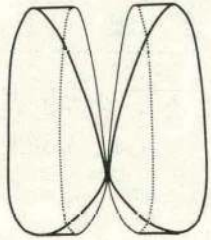
$$X^2 + (Y + 6)^2 \geq (0.876)^2,$$

$$Y + 6 \leq 0,$$

$$67.2 \leq Z \leq 71.58,$$

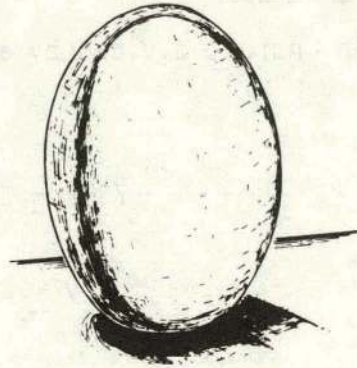


TOP VIEW

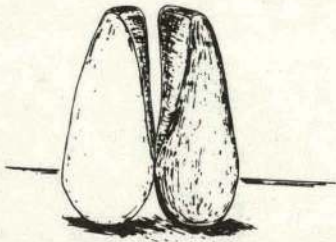


FRONT VIEW

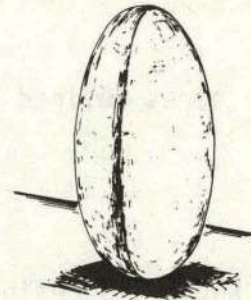
THYROID



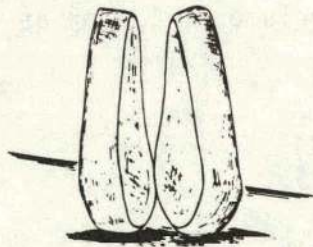
TESTIS



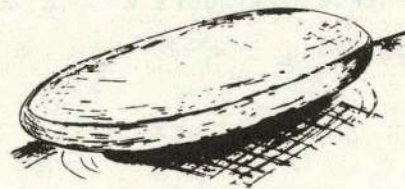
THYROID



OVARY



THYROID



THYMUS

FIGURE A-2. MATHEMATICAL MODELS FOR THE THYROID, TESTIS, OVARIES AND THYMUS.

and

$$\left[(Y + A) - |X| \right]^2 \geq Z \left[X^2 + (Y + A)^2 \right] \tau^2,$$

in which

$$\tau = \frac{2(\sqrt{2} - 2)}{4.38} (Z - 67.2) + 1 \quad \text{for } 0 \leq Z - 67.2 \leq 1.095$$

or

$$\tau = \frac{2(2 - \sqrt{2})}{13.14} (Z - 67.2) + \frac{2\sqrt{2} - 1}{3} \quad \text{for } 1.095 \leq Z - 67.2 \leq 4.38.$$

The upper spine (Figure 2, page 13) is an elliptical cylinder with a volume of 102 cm³ defined by

$$\left(\frac{X}{1.9} \right)^2 + \left(\frac{Y - 5.5}{2.3} \right)^2 \leq 1, \quad 67.2 \leq Z \leq 75.63.$$

The trunk section (Figure 1, page 12) is described as a right elliptical cylinder with a total mass of 34.3 kg and a volume of 34,834 cm³. It is the principal section in which most internal organs lie and is defined by

$$\left(\frac{X}{16.5} \right)^2 + \left(\frac{Y}{10} \right)^2 \leq 1, \quad 0 \leq Z \leq 67.2.$$

The middle spine (Figure 2, page 13) connects to the upper and lower spine all described by the same elliptical cylinder. The middle and lower portions have volumes of 469 cm³ and 173 cm³ respectively. The defining equations are

$$\left(\frac{X}{1.9} \right)^2 + \left(\frac{Y - 5.5}{2.3} \right)^2 \leq 1,$$

where

$$33.07 \leq Z < 67.2 \quad \text{for the middle spine}$$

and

$$20.53 \leq Z \leq 33.07 \quad \text{for the lower spine.}$$

The arm bones (Figure 8, page 23) are frustrums of elliptical cones having a combined volume of 801 cm³ defined by

$$\left[\frac{(1.31/132.4)(Z-66.2) + (X \pm 14.99)}{1.31} \right]^2 + \left(\frac{Y}{2.52} \right)^2 \leq \left[\frac{132.4 + (Z-66.2)}{132.4} \right]^2,$$

and

$$0 \leq Z \leq 66.2.$$

The ribs (Figure A-3) are represented as a series of bands between two concentric, right elliptical cylinders. They are equispaced and have a total volume of 581 cm³ defined by

$$\left(\frac{X}{13.5} \right)^2 + \left(\frac{Y}{9.8} \right)^2 \leq 1,$$

$$\left(\frac{X}{13.0} \right)^2 + \left(\frac{Y}{9.3} \right)^2 \geq 1,$$

and

$$33.7 \leq Z \leq 64.81,$$

where the integral part of $\left(\frac{Z-33.7}{1.353} \right)$ must be even.

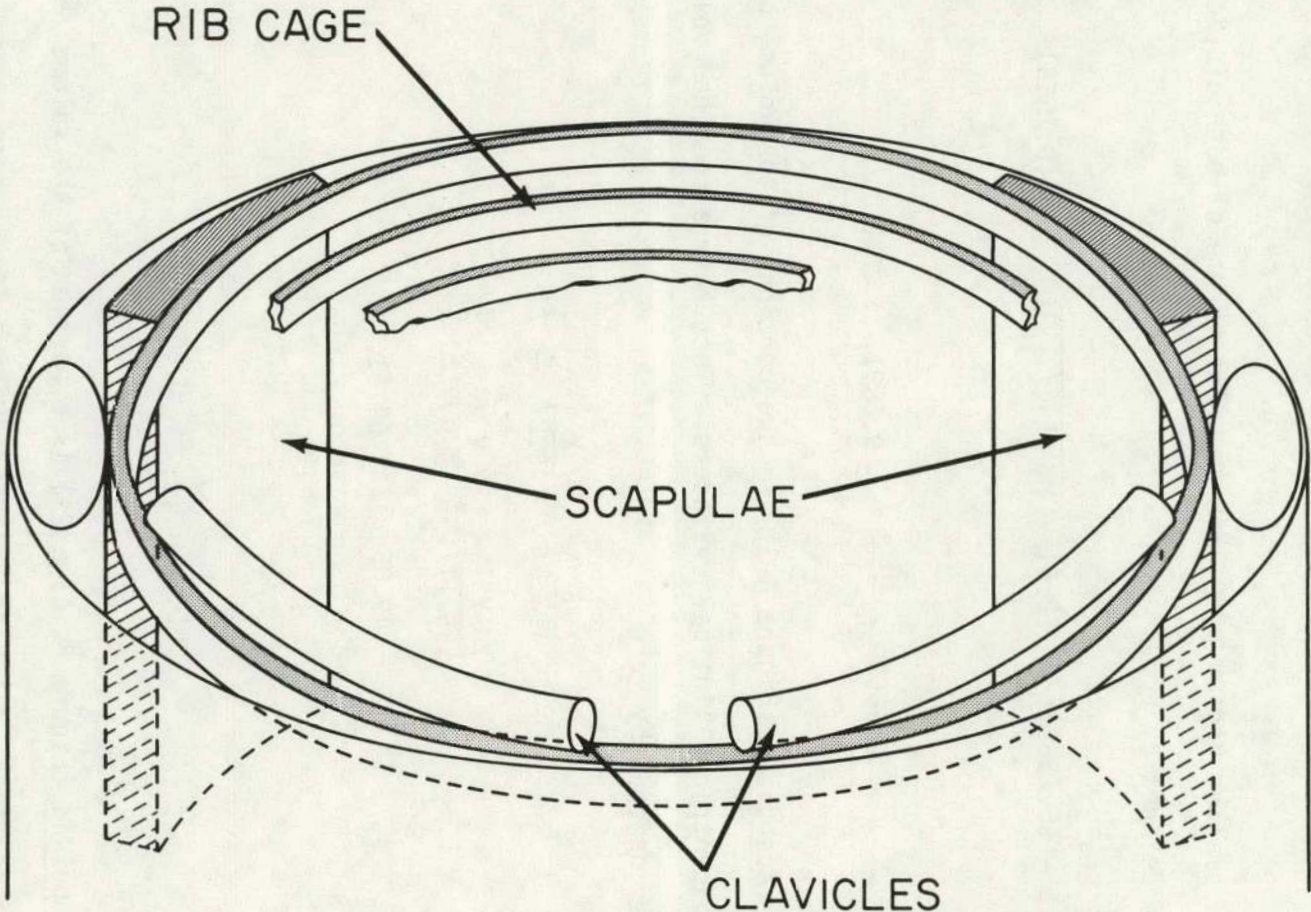


FIGURE A-3. DETAILED VIEW OF SCAPULAE AND CLAVICLES.

The clavicles (Figure A-3) are represented as two portions of a focus which lie along the circular arc

$$X^2 + (Y - 10)^2 = (18.61)^2, \quad Z = 65.7568,$$

and has a smaller radius of 0.7568 cm. The volume of both clavicles is 46 cm^3 as defined by

$$(Z - 65.7568)^2 + 18.61 - \sqrt{X^2 + (Y - 10)^2} \leq (0.7568)^2,$$

and

$$0.96569 \leq \frac{10 - Y}{|X|} \leq 9.6891, \quad Y \leq 0.$$

The scapulae (Figure A-3) are two portions of the volume between two nonconcentric elliptical cylinders. They have a combined volume of 170 cm^3 as defined by

$$\left(\frac{X}{13.5}\right)^2 + \left(\frac{Y}{9.8}\right)^2 \geq 1,$$

$$\left(\frac{X}{15.11}\right)^2 + \left(\frac{Y}{9.8}\right)^2 \leq 1,$$

$$49.05 \leq Z \leq 64.81,$$

$$Y > 0,$$

and

$$0.25 < \frac{Y}{|X|} < 0.80.$$

The pelvis (Figure 8, page 23) is a portion of the volume between two nonconcentric circular cylinders with a total organ volume of 508 cm^3 defined by

$$\begin{aligned} X^2 + (Y + 3)^2 &\leq (11.2)^2, \\ X^2 + (Y + 3.8)^2 &\geq (10.6)^2, \\ Y + 3 &\geq 0, \\ 0 &\leq Z \leq 20.53, \end{aligned}$$

and

$$Y \leq 5 \quad \text{if} \quad Z \leq 13.03.$$

The idealization used to represent the gastrointestinal tract is shown in Figure A-4. The stomach is the volume between two ellipsoids. The stomach wall is 0.56 cm thick and has a volume of 118 cm³. The contents within the stomach occupy a volume of 193 cm³. The defining equations are

$$\left(\frac{X - 6}{3.67}\right)^2 + \left(\frac{Y + 4}{2.75}\right)^2 + \left(\frac{Z - 33.6}{7.35}\right)^2 \leq 1,$$

and

$$\left(\frac{X - 6}{3.107}\right)^2 + \left(\frac{Y + 4}{2.187}\right)^2 + \left(\frac{Z - 33.6}{6.777}\right)^2 \geq 1.$$

The small intestine is regarded as occupying a volume within which it is free to move. No attempt has been made to distinguish between the wall and contents within the volume. The total volume of both wall and contents is 752 cm³ and is located within the section of a circular cylinder defined by

$$X^2 + (Y + 3.8)^2 \leq (10.6)^2,$$

$$-4.67 \leq Y \leq 2.2,$$

ORNL-DWG 73-12124

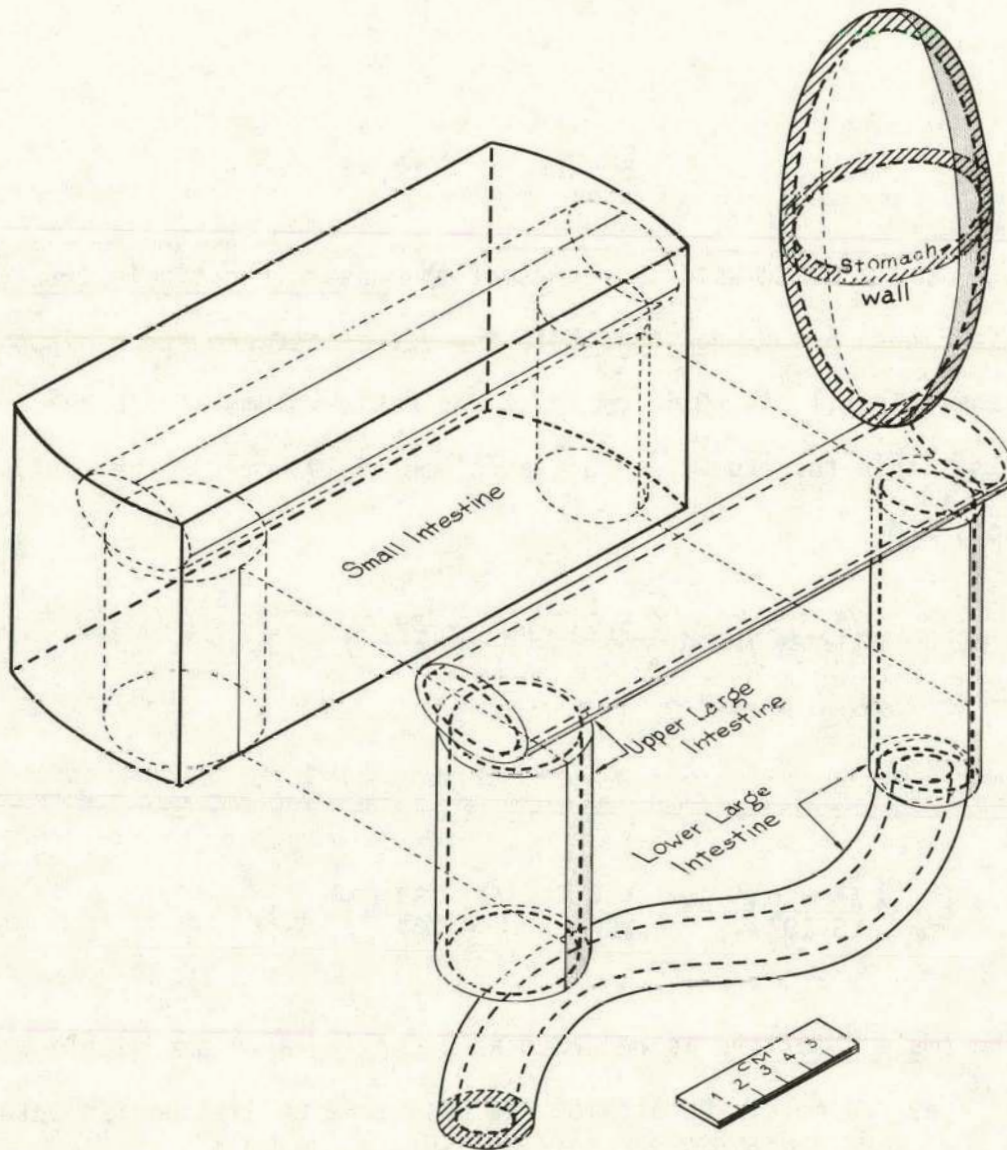


FIGURE A-4. GASTROINTESTINAL TRACT.

and

$$18.25 \leq Z \leq 26.25.$$

The upper large intestine has two sections, an ascending colon and a transverse colon. The ascending colon wall is the volume between two circular cylinders. The wall volume is 64 cm^3 and the content volume is 67 cm^3 . The wall is defined by

$$(X + 7)^2 + (Y + 2.36)^2 \leq (2.13)^2,$$

$$(X + 7)^2 + (Y + 2.36)^2 \geq (1.5264)^2,$$

and

$$13.8 \leq Z \leq 23.$$

The wall of the transverse colon is the space between two elliptical cylinders and has a volume of 85 cm^3 . The volume of the contents is 89 cm^3 . The wall is defined by

$$\left(\frac{Y + 2.36}{2.13}\right)^2 + \left(\frac{Z - 24.5}{1.5}\right)^2 \leq 1,$$

$$\left(\frac{Y + 2.36}{1.632}\right)^2 + \left(\frac{Z - 24.5}{1.002}\right)^2 \geq 1,$$

and

$$-8.63 \leq X \leq 8.63.$$

The lower large intestine consists of a descending colon and a sigmoid colon. The contents of the descending colon has a volume of 71 cm^3 . The volume of the wall is 63 cm^3 as defined by

$$\left(\frac{X - X_0}{1.602}\right)^2 + \left(\frac{Y - Y_0}{1.815}\right)^2 \leq 1,$$

$$\left(\frac{X - X_0}{1.346}\right)^2 + \left(\frac{Y - Y_0}{1.141}\right)^2 \geq 1,$$

and

$$8.3 \leq Z \leq 23,$$

where

$$X_0 = 8.5 + \frac{0.2(7 - 23)}{14.7},$$

and

$$Y_0 = \frac{2.5(8.3 - Z)}{14.7}.$$

The contents of the sigmoid colon has a volume of 25 cm³. The wall consists of portions of two torii and has a volume of 49 cm³ as defined by

$$\left(\sqrt{(X - 2.86)^2 + (Z - 8.3)^2} - 5.44\right)^2 + Y^2 \leq (1.3457)^2,$$

$$\left(\sqrt{(X - 2.86)^2 + (Z - 8.3)^2} - 5.44\right)^2 + Y^2 \geq (0.7801)^2,$$

$$X \geq 2.86 \quad \text{and} \quad Z \leq 8.72,$$

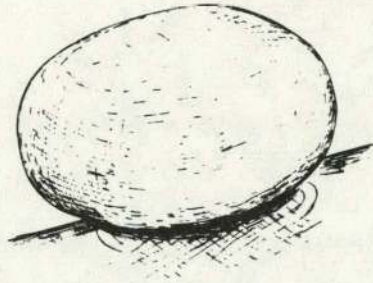
and

$$\left(\sqrt{(X - 2.86)^2 + Z^2} - 2.86\right)^2 + Y^2 \leq (1.3457)^2,$$

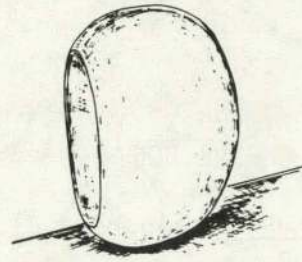
$$\left(\sqrt{(X - 2.86)^2 + Z^2} - 2.86\right)^2 + Y^2 \geq (0.7801)^2,$$

$$X \leq 2.86 \quad \text{and} \quad Z \geq 0.$$

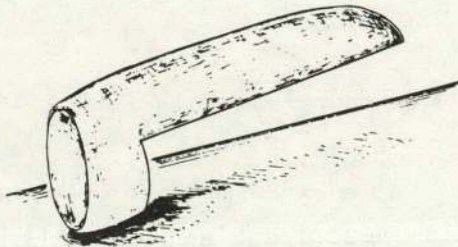
The urinary bladder (Figure A-5) is an ellipsoid. The volume of the contents is 155 cm³ and the volume of the wall is 35 cm³ as defined by



BLADDER



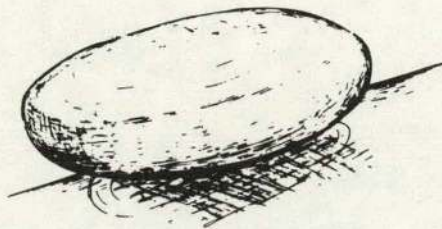
KIDNEY



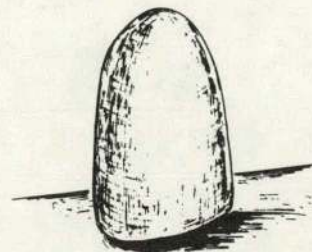
PANCREAS



UTERUS



SPLEEN



ADRENAL

FIGURE A-5. MATHEMATICAL MODELS FOR BLADDER, KIDNEYS, PANCREAS, UTERUS, SPLEEN AND ADRENALS.

$$\left(\frac{X}{4.536}\right)^2 + \left(\frac{Y + 4.5}{3.163}\right)^2 + \left(\frac{Z - 7.68}{3.163}\right)^2 \leq 1,$$

and

$$\left(\frac{X}{4.306}\right)^2 + \left(\frac{Y + 4.5}{2.933}\right)^2 + \left(\frac{Z - 7.68}{2.933}\right)^2 \geq 1.$$

The uterus (Figure A-5) is an ellipsoid cut by a plane with a total volume of 29 cm³ defined by

$$\left(\frac{X}{1.9}\right)^2 + \left(\frac{Y + 2}{3.81}\right)^2 + \left(\frac{Z - 13}{1.14}\right)^2 \leq 1, \quad Y \geq -3.91.$$

The ovaries (Figure A-2, page 60) are ellipsoids with a combined volume of about 5 cm³ defined by

$$\left(\frac{X \pm 4.95}{0.856}\right)^2 + \left(\frac{Y}{0.428}\right)^2 + \left(\frac{Z - 14.5}{1.713}\right)^2 \leq 1.$$

The liver (Figure A-1, page 58) is described as an elliptical cylinder cut by a plane with a total volume of 1284 cm³ defined by

$$\left(\frac{X}{13}\right)^2 + \left(\frac{Y}{8}\right)^2 \leq 1,$$

$$\frac{X}{32.31} + \frac{Y}{41.54} - \frac{Z}{42} \leq -1,$$

and

$$26.25 < Z \leq 42.$$

The pancreas (Figure A-5) is half an ellipsoid with a section removed with a total volume of 57 cm³ defined by

$$\left(\frac{X}{12.8}\right)^2 + \left(\frac{Y}{1.047}\right)^2 + \left(\frac{Z - 35.52}{3.141}\right)^2 \leq 1,$$

$$X \geq 0,$$

and

$$Z \geq 35.52 \quad \text{if} \quad X \geq 2.56.$$

The spleen (Figure A-5) is an ellipsoid with a volume of 145 cm³ defined by

$$\left(\frac{X - 8.5}{3.28}\right)^2 + \left(\frac{Y - 3}{1.88}\right)^2 + \left(\frac{Z - 35.52}{5.63}\right)^2 \leq 1.$$

The kidneys (Figure A-5) are each described as an ellipsoid cut by a plane with the combined volume of 236 cm³ as defined by

$$\left(\frac{X \pm 5.5}{4.212}\right)^2 + \left(\frac{Y - 6}{1.404}\right)^2 + \left(\frac{Z - 31.4}{5.147}\right)^2 \leq 1,$$

and

$$X \geq 2.69.$$

The adrenals (Figure A-5) are half ellipsoids located one on top of each kidney. The volume of both adrenals is about 9 cm³, defined by

$$\left(\frac{X \pm 4.743}{1.257}\right)^2 + \left(\frac{Y - 6.419}{0.419}\right)^2 + \left(\frac{Z - 36.6}{4.189}\right)^2 \leq 1,$$

and

$$Z \geq 36.6.$$

Each lung (Figure A-1, page 58) is half an ellipsoid with an anterior section removed. The volume of both lungs is 2167 cm³ and the defining equations are

$$\left(\frac{X - 7}{4.312}\right)^2 + \left(\frac{Y}{6.468}\right)^2 + \left(\frac{Z - 42.25}{20.698}\right)^2 \leq 1,$$

$$Z \geq 42.25$$

and

$$\left(\frac{X - 1.82}{4.312}\right)^2 + \left(\frac{Y}{6.468}\right)^2 + \left(\frac{Z - 42.25}{20.698}\right)^2 \geq 1 \quad \text{if } Y < 0.$$

The heart (Figure A-1, page 58) is half an ellipsoid capped by a hemisphere which is cut by a plane. The volume of the heart is 241 cm³. The axes of the ellipsoids describing the heart are not parallel to the X, Y, and Z axes. The equations defining the rotation and translation, as well as the heart volume, are

$$X_1 = 0.6943(X + 0.825) - 0.3237(Y + 2.59) - 0.6428(Z - 49),$$

$$Y_1 = 0.4226(X + 0.825) + 0.9063(Y + 2.59),$$

$$Z_1 = 0.5826(X + 0.825) - 0.2717(Y + 2.59) + 0.766(Z - 49),$$

$$\left(\frac{X_1}{5.892}\right)^2 + \left(\frac{Y_1}{3.682}\right)^2 + \left(\frac{Z_1}{3.682}\right)^2 \leq 1,$$

and $X_1^2 + Y_1^2 + Z_1^2 \leq (3.682)^2$ if $X_1 < 0$,

$$\left(\frac{X_1}{2.22}\right) + \left(\frac{Z_1}{3.682}\right) \geq -1 \quad \text{if } X_1 < 0.$$

The thymus (Figure A-2, page 60) is an ellipsoid with a volume of 27 cm³ as defined by

$$\left(\frac{X + 2}{3.086}\right)^2 + \left(\frac{Y + 6}{0.514}\right)^2 + \left(\frac{Z - 58.1}{4.115}\right)^2 \leq 1.$$

The legs section (Figure 1, page 12) has two major regions which are the legs region and the genitalia region. The genitalia region has a total volume of 154 cm³ and is considered to be soft tissue. The region is defined by

$$-4.55 \leq Z \leq 0,$$

$$-(8.25 + \frac{Z}{12.128}) \leq Z \leq (8.25 + \frac{Z}{12.128}),$$

$$-(10 + \frac{Z}{9.475}) \leq Y \leq 0,$$

and

$$\left[\left(\frac{X}{(8.25 + Z/12.128)} \right) \pm 1 \right]^2 + \left[\frac{Y}{(10 + Z/9.475)} \right]^2 \geq 1.$$

The testicles (Figure A-2, page 60) are ellipsoids with a combined volume of about 16 cm³ as defined by

$$\left(\frac{X \pm 0.973}{0.973} \right)^2 + \left(\frac{Y + 7.6}{1.123} \right)^2 + \left(\frac{Z + 1.722}{1.722} \right)^2 \leq 1.$$

The legs region consists of the frustrums of two elliptical cones with a total volume of 16,630 cm³ and a total mass of about 17.5 kg.

The defining equations for the leg region are

$$\left[\left(\frac{Z}{(8.25 + Z/12.128)} \right) \pm 1 \right]^2 + \left[\frac{Y}{(10 + Z/9.475)} \right]^2 \leq 1,$$

and

$$-75.8 \leq Z \leq 0.$$

The leg bones (Figure 8, page 23) are frustrums of elliptical cones with a combined volume of 2,231 cm³ as defined by

$$\left[X \pm \left(8.25 + \frac{6.25}{75.6} Z \right) \right]^2 + Y^2 \leq \left(3.152 + \frac{2.152}{75.6} Z \right)^2,$$

and

$$-75.6 \leq Z \leq 0.$$

APPENDIX B

ASSUMPTIONS FOR ^{99m}Tc -DMSA

(2, 3-DIMERCAPTORUCCING ACID)

Certain assumptions had to be made in formulating the biological model for the administration of ^{99m}Tc -DMSA. The assumptions and distributions used in the calculations associated with this particular radiopharmaceutical were as follows:

1. 60% of the administered activity localized instantaneously in the renal cortices with $T_{\frac{1}{2}B}$ much larger than $T_{\frac{1}{2}phy}$; i.e., $T_{eff} = T_{phy}$. The ratio of the cortical tissue in the adult to total renal tissue is $186/300 = 0.62$ and remains the same for the fifteen year-old.

2. 33% of the administered activity distributed itself instantaneously and uniformly throughout the total body with a $T_{\frac{1}{2}B} \gg T_{phy}$; i.e., $T_{eff} = T_{phy}$.

3. 5% of the administered activity localized instantaneously in the liver and spleen (proportional to organ mass) with a $T_{\frac{1}{2}B} \gg T_{phy}$; i.e., $T_{eff} = T_{phy}$.

4. 2% of the administered activity was cleared by the kidneys and the effective residence time of the activity in the bladder is one hour. Physical decay was not considered. (The value of 2% excretion was taken to err on the low side, thus increasing the estimate of tissue radiation dose has retained activity).

5. There was no free ^{99m}Tc and all of the ^{99m}Tc activity followed the kinetics of the renal agent.

These assumptions have been taken in their entirety from the work of Dr. E. M. Smith as used in work with the children phantoms.¹⁸

APPENDIX C

DERIVATION OF A_r

The cumulative activity, \tilde{A} ($\mu\text{Ci-h}$), is the time integral of the total activity $A(t)$. There are processes determining the activity in the body at any time; the physical decay of the radionuclide, the biological elimination of the radionuclide. Therefore,

$$A(t) = A(0) e^{-\lambda t} q(t) \quad \mu\text{Ci} \quad (1)$$

where

$A(0)$ = the initial activity of the radionuclide (μCi).

λ = the physical decay constant.

$q(t)$ = the fractional amount of the administered radionuclide in a region at any time t .

The assumption was made that for absorbed dose calculations, $q(t)$ can be expressed as the sum of a number of exponential components,³⁷ such that,

$$q(t) = \sum_j q_j e^{-\lambda_j t} \quad (2)$$

where the λ_j 's are the biological decay constants. This yields

$$A(t) = A(0) e^{-\lambda t} \sum_j q_j e^{-\lambda_j t}$$

and

$$A(t) = A(0) \sum_j q_j e^{-[\lambda + \lambda_j]t} \quad (3)$$

If

$$A = \int_0^t A(t) dt \quad (4)$$

then

$$\tilde{A} = A(0) \sum_j \frac{q_j}{\lambda + \lambda_j} \left[1 - e^{-[\lambda + \lambda_j]t} \right] \quad (5)$$

Taking the limit of equation (5) as t approaches ∞ gives

$$\tilde{A}(\infty) = A(0) \sum_j \frac{q_j}{\lambda + \lambda_j} (\mu\text{Ci-h}) \quad (6)$$

The assumption was made in formulating the biological model, that the time for biological clearance of the radionuclide is much larger than the physical half-life. This means that

$$\lambda \gg \lambda_j.$$

The summation of q_j over all j 's is equal to the total fraction of the administered radionuclide in that region. Let this fraction for any region r be q_r and the cumulated activity, assumed to be uniformly distributed in any region r , is then

$$\tilde{A}_r = A(0) \frac{q_r}{\lambda} \mu\text{Ci-h}. \quad (7)$$

It is convenient to cast the cumulated activity in units of $\mu\text{Ci-h}$ per μCi of administered activity. This is obtained by assuming that $A(0)$ has a value of 1 μCi of administered activity and dividing both sides of equation (7) by $A(0)$ to obtain the final equation for the cumulated activity

$$\tilde{A}_r' = \frac{q_r}{\lambda} \mu\text{Ci-h}/\mu\text{Ci administered}.$$

APPENDIX D
THE MONTE CARLO TECHNIQUE

The computer code GAM-15 incorporates the geometry of the fifteen year-old in a Monte Carlo gamma-ray transport code. The original code, OGRE³⁴, has been used with the geometry of the adult phantom to form a new code, ALGAM³⁵, which is used to estimate absorbed doses. GAM-15 was developed in this same manner. Therefore, the Monte Carlo technique employed remains unchanged. The description below can be found in Snyder et al.¹⁶ and a similar description is in MIRD Pamphlet Number 5.³⁰

"Photon histories are determined using the mass-attenuation coefficients $\mu_{pe}(E)$, $\mu_c(E)$ and $\mu_{pp}(E)$ for the photoelectric, Compton and pair production interactions, respectively. Because these were calculated from atomic attenuation coefficients tabulated in NBS Circular 583 (Grodstein, 1957; McGinnis, 1959)* and compositions listed in Table A-1,** they have different values for regions with differing compositions. The procedure for using these coefficients was not the straightforward one of obtaining an interaction site and then tracing back along the path to find the first surface where the photon entered a medium whose attenuation coefficient differed from that of the region where it began the flight. This method would have entailed a considerable increase in computer time. Instead, for the first step of

* See references 38 and 39.

** The elemental composition of the fifteen year-old was assumed the same as that of the adult. For this table, see reference 16, page 26.

the procedure, an attenuation coefficient μ_0 was used that was greater than or equal to that of any of the regions, i.e., skeletal, lung and the remainder of the phantom. The potential site of an interaction was chosen by the usual procedure of taking the distance traversed as

$$\text{distance} = (-\ln r)/\mu_0$$

in which r is a number distributed randomly between 0 and 1. The point on the line at this distance from the starting point in the direction of the photon's path was then tested to determine the region of the phantom containing it. Denoting this region by i , one then plays a game of chance with probability μ_i/μ_0 of acceptance where μ_i is the total mass-attenuation coefficient for the region. If the outcome of the game is favorable, the interaction site is accepted; if it is unfavorable, the photon is allowed another flight beginning at the point reached and continuing with the same direction and energy. It is not difficult to prove that this procedure gives a photon the correct expectation of reaching any point on the line regardless of how many boundaries it crosses.

"In addition to scattering, the photons have a finite probability of absorption which predominates at low energies. Thus very few photons will penetrate to large distances, and therefore the statistics of the estimate will be poor. To compensate partially for this, each photon was given a weight that initially was set at unity. With each interaction, this weight was reduced to allow for the probability of survival, and the photon was allowed to continue undergoing only Compton scattering interactions. The reduction of weight is expressed by

$$W_n = W_{n-1} \frac{\mu_c(E_{n-1})}{\mu(E_{n-1})}$$

in which W_n is the weight carried by the photon after the n^{th} collision and $\mu_c(E_{n-1})$ and $\mu(E_{n-1})$ are the coefficients for Compton scattering and the total coefficient before the n^{th} collision, respectively. This reduction of the weight carried by the photons is equal to the expectation of a Compton scattering which the photon would have in the actual physical processes. The total flight history of a photon is terminated (1) if it escapes from the phantom, (2) if its energy falls below 4 keV or (3) if its weight falls below 10^{-5} ; in the latter two cases, the energy was considered as locally absorbed.

"The energy deposition for the n^{th} interaction, E_n^* , is

$$E_n^* = W_{n-1} \left[\frac{\mu_{pe}(E_{n-1})}{\mu(E_{n-1})} E_{n-1} + \frac{\mu_c(E_{n-1})}{\mu(E_{n-1})} (E_{n-1} - E_n) + \frac{\mu_{pp}(E_{n-1})}{\mu(E_{n-1})} (E_{n-1} - 2m_0c^2) \right]$$

in which $\mu_{pe}(E_{n-1})$, $\mu_c(E_{n-1})$ and $\mu_{pp}(E_{n-1})$ are the mass-attenuation coefficients for the photoelectric, Compton and pair-production processes before the collision at the site considered, respectively, and m_0c^2 is the rest mass energy of an electron. It will be noted that the total energy of the photon is absorbed locally when a photoelectric process occurs, and this is also the case for the kinetic energy of the electron and positron produced by pair production. The positron will be annihilated, and two photons of energy m_0c^2 (≈ 0.51 MeV) will be emitted. The computer code is designed to take account of these photons since a new photon energy of 0.51 MeV with weight

$$2W_{n-1} \mu_{pp}(E_{n-1}) / \mu(E_{n-1}),$$

and a random orientation is started at the site of the pair production and followed independently afterward.

"No procedure has been used to take account of the finite range of the electrons and positrons that are produced. Generally, these ranges are small compared with the diameters of most organs, and the absorbed dose will not change abruptly with distance except at a boundary where composition and density change or at the boundary of the source organ. At such a boundary the density of photon interactions may change abruptly. The change in absorbed dose would be somewhat less abrupt at such a boundary due to the finite range of the secondary particles. Thus neglect of this further dispersion of the energy distribution in this calculation accentuates the change of absorbed dose at such a boundary. However there is no attempt here to estimate boundary effects. We estimated only an absorbed fraction for each organ considered as a whole.

"Finally bremsstrahlung might be considered as a further example of a secondary form of radiation which might have a rather extended range, and so these photons might be followed by the Monte Carlo method. This has not been done, first, because the probability of producing a photon with an energy approaching the kinetic energy of the electron is rather small--although greater than zero--and, second, because the total energy accounted for by bremsstrahlung is very small for the energies and materials considered here (NAS-NRC, 1964).[†]

Statistics

"A standard deviation of each estimate has been calculated. The following discussion will describe the procedure used for each region. Let E_{ni}^* be the energy deposited in the region under consideration on the n^{th} interaction of the i^{th} source photon. This energy may be zero,

[†]See reference 40.

as it will be in the frequently occurring case when the n^{th} interaction does not occur within the region. The total energy deposited by the i^{th} photon, or by the i^{th} history, to the region will be

$$E_i^* = \sum_{n=1}^{m_i} E_{ni}^*$$

in which m_i is the number of interactions occurring in the i^{th} history before termination. The estimate of the average energy deposited per photon in the region is the

$$\bar{E} = \frac{1}{M} \sum_{i=1}^M E_i^*$$

in which M source photons were followed.

"For the standard deviation, σ , of the estimate \bar{E} , one has

$$\sigma^2 = \frac{1}{M(M-1)} \sum_{i=1}^M (E_i^* - \bar{E})^2.$$

Since the absorbed fraction and specific absorbed fraction will differ from \bar{E} by constant factors, they will have a coefficient of variation, CV, which is the same as that for \bar{E} . Thus $CV = 100\sigma/\bar{E}$ in percent, and in this formulation it is also the coefficient of variation of the absorbed fraction and the specific absorbed fraction.

"When the distribution of \bar{E} is known to be approximately normal, one can determine a confidence interval by using the standard deviation. However, there are several indications that \bar{E} is not normally distributed in cases where the coefficient of variation is greater than 50%. This generally occurs when there are fewer than 100 interactions contributing to the estimated absorbed fraction. Under these circumstances σ cannot be used to estimate confidence intervals

as is customary when the sample is normally distributed. A small number of interactions may occur in a region that has a small volume or that is many mean-free flight paths from the source. Sometimes both conditions may apply. The computer records the number of photons that have an interaction in each region, and this has been examined also to estimate subjectively the accuracy of the estimate.

"Examination of results in cases where the coefficient of variation exceeds 50%, often compared with results of independent recalculation of such estimates, leads us to believe that the estimate may often be in error by a factor of 2 to 5. . . Values obtained by the Monte-Carlo-type calculation are estimates based on the sample size of 60,000 photons."

INTERNAL DISTRIBUTION

- | | | | |
|--------|-------------------------------------|--------|-----------------|
| 1-2. | Central Research Library | 43. | D. G. Jacobs |
| 3. | Document Reference Section | 44. | T. D. Jones |
| 4-6. | Laboratory Records Department | 45. | G. D. Kerr |
| 7. | Laboratory Records, ORNL R.C. | 46. | S. K. Penny |
| 8. | ORNL Patent Office | 47-71. | J. W. Poston |
| 9. | Research and Technical Support Div. | 72. | C. R. Richmond |
| 10-36. | Technical Information Center | 73. | R. L. Shoup |
| 37. | J. A. Auxier | 74. | W. S. Snyder |
| 38. | S. R. Bernard | 75. | P. S. Stansbury |
| 39. | M. F. Fair | 76. | S. B. Watson |
| 40. | M. R. Ford | 77. | G. G. Warner |
| 41. | F. F. Haywood | 78. | H. A. Wright |
| 42. | J. L. Hwang | | |

EXTERNAL DISTRIBUTION

79. S. James Adelstein, Shields Warren Radiology Lab., 50 Binney St., Boston, Mass. 02115.
80. Monte Blau, Roswell Park Memorial Institute, Dept. of Nuclear Medicine, 666 Elm Street, Buffalo, NY 14203.
81. Mones Berman, National Cancer Institute of Health, Building 10, Room 4B-56, Bethesda, MD 20014.
82. C. E. Carter, Division of Biomedical and Environmental Research, ERDA, Washington, D. C. 20545.
83. R. J. Cloutier, ORAU, Oak Ridge, Tennessee 37830.
84. R. D. Cooper, Division of Biomedical and Environmental Research, ERDA, Washington, D. C. 20545.
85. Dr. George Cowper, Atomic Energy of Canada, Ltd., Chalk River, Ontario, Canada.
86. L. J. Deal, Asst. Director of Safety Protection, Division of Operational Safety, ERDA, Washington, D. C. 20545.
87. L. T. Dillman, Department of Physics, Ohio Wesleyan University, Delaware, Ohio 43015.
88. A. K. Furr, Nuclear Science Engineering Dept., Virginia Polytechnic Institute and State University, Blacksburg, Virginia 24060.
- 89-93. R. M. Jones, Mechanical Engineering Dept., Virginia Polytechnic Institute and State University, Blacksburg, Virginia 24060.
94. H. A. Kurstedt, Nuclear Science Engineering Dept., Virginia Polytechnic Institute and State University, Blacksburg, Virginia 24060.
95. Marguerite T. Hays, 151, Director of Medical Research Services, Veterans Administration, Department of Medicine and Surgery, Washington, D. C. 20420.

EXTERNAL DISTRIBUTION (CONT'D)

96. R. Eugene Johnston, Dept. of Radiology, NCMH, Division of Nuclear Medicine, University of North Carolina, Chapel Hill, N.C. 27514.
97. Dr. James Kereiakes, E555 Medical Sciences Building, University of Cincinnati, Cincinnati, Ohio 45267.
98. Katherine A. Lathrop, Franklin McLean Memorial Research Institute, The Univ. of Chicago, 950 East 59th St., Box 420, Chicago, Ill. 60637.
99. Robert Loevinger, Radiation Physics Bldg., Room C210, National Bureau of Standards, Washington, D. C. 20234.
100. John G. McAfee, Division of Nuclear Medicine, Upstate Medical Center, 750 East Adams Street, Syracuse, NY 13210.
101. K. Z. Morgan, School of Nuclear Engineering, Georgia Institute of Technology, Atlanta, GA 30332.
102. Dr. Peter Paras, Bureau of Radiological Health, Food and Drug Administration, 12720 Twinbrook Parkway, Rockville, MD 20852.
103. D. B. Rivers, Nuclear Science Engineering Dept., Virginia Polytechnic Institute and State University, Blacksburg, VA 24060.
104. Robert H. Rohrer, Dept. of Physics, Emory University, Atlanta, GA 30322.
105. Marvin Rosenstein, Bureau of Radiological Health, Food and Drug Administration, 12720 Twinbrook Parkway, Rockville, MD 20852.
106. Edward M. Smith, Executive Director, MIRD Committee, 404 Church Street, Suite 15, Maryville, TN 37801.
107. L. V. Spencer, Center on Radiation Research, National Bureau of Standards, Washington, D. C. 20234.
108. Betsy J. Stover, Division of Health Affairs, Department of Pharmacology, Swing Building, University of North Carolina, Chapel Hill, N.C. 27514.
109. John C. Villforth, Bureau of Radiological Health, Food and Drug Administration, 12720 Twinbrook Parkway, Rockville, MD 20852.
110. Robert W. Wood, Division of Biomedical and Environmental Research, Radiological Physics and Instrumentation Branch, ERDA, Washington, D.C. 20545.